Interleukin-1α (IL-1α) is a central regulator of inflammation in cardiovascular and kidney diseases

Authors

Stefan J Schunk, MD[1]; Sarah Triem, MSc[1,2]; David Schmit, MD[1]; Stephen Zewinger, MD[1]; Tamim Sarakpi, MD[1]; Ellen Becker, BS[1,2]; Gregor Hütter, MD[1,2]; Selina Wrublewsky, MSc[3]; Mathias Hohl, PhD[4]; Dalia Alansary, PhD[5]; Leticia Prates Roma, PhD[5]; Peter Lipp, PhD[6]; Julia Möllmann, PhD[7]; Michael Lehrke, MD[7]; Matthias W. Laschke, MD PhD[3]; Michael D Menger, MD[3]; Rafael Kramann, MD PhD[8,9]; Peter Boor, MD PhD[10]; Willi Jahnen-Dechent, PhD[11]; Michael Böhm, MD[4]; Ulrich Laufs, MD[12]; Barbara A. Niemeyer, PhD[5]; Danilo Fliser, MD[1]; Emmanuel Ampofo, PhD[3]*; Thimoteus Speer, MD PhD[1,3]*

Affiliations

1 Department of Internal Medicine IV, Nephrology and Hypertension, Saarland University, Homburg/Saar, Germany

2 Translational Cardiorenal Medicine, Saarland University, Homburg/Saar, Germany

3 Institute of Clinical and Experimental Surgery, Saarland University, Homburg/Saar, Germany

4 Department of Internal Medicine III, Cardiology, Angiology, and Intensity Care Medicine, Saarland University, Homburg/Saar, Germany

5 Institute of Biophysics, CIPMM, Saarland University, Homburg/Saar, Germany

6 Institute of Cell Biology, Saarland University, Homburg/Saar, Germany

7 Department of Cardiology, RWTH Aachen University Hospital, Aachen, Germany

8 Department of Nephrology, RWTH Aachen University Hospital, Aachen, Germany

9 Institute of Experimental Medicine and Systems Biology, RWTH Aachen, Aachen, Germany

10 Institute of Pathology, RWTH Aachen University Hospital, Aachen, Germany

11 Biointerface Laboratory, RWTH Aachen University Hospital, Aachen, Germany

12 Department of Cardiology, University Hospital Leipzig, Leipzig, Germany

* Both authors contributed equally

Corresponding author

Thimoteus Speer, MD PhD

Saarland University

Translational Cardio-Renal Medicine

Building 41, IMED

66424 Homburg/Saar

Germany

Phone : +49 6841 16 15048

E-Mail: timo.speer@uks.eu

Keywords

Interleukin-1α, inflammation, leukocyte adhesion, myocardial infarction, chronic kidney disease

Word count

4,975

Abstract

Background

Cardiovascular diseases (CVD) and chronic kidney disease (CKD) are highly prevalent, aggravate each other, and account for substantial mortality. Both conditions are characterized by activation of the innate immune system. The alarmin IL-1α is expressed in a variety of cell types promoting (sterile) systemic inflammation. The aim of the present study is to examine the role of IL-1α in mediating inflammation in the setting of cardiorenal diseases.

Methods

We assessed the expression of IL-1α on the surface of monocytes from patients with acute myocardial infarction (AMI) and patients with CKD and determined its association with atherosclerotic CVD events during follow-up in an explorative clinical study. Furthermore, we assessed the inflammatory effects of IL-1α in several organ injury models in *Il1a*$^{-/-}$ and *Il1b*$^{-/-}$ mice and investigated the underlying mechanisms *in vitro* in monocytes and endothelial cells.

Results

IL-1α is strongly expressed on the surface of monocytes from patients with AMI and CKD compared to healthy controls. Higher IL-1α surface expression on monocytes from patients with AMI was associated with a higher risk for atherosclerotic CVD events, which underlines the clinical relevance of IL-1α. In mice, IL-1α, but not IL-1β, mediates leukocyte-endothelial adhesion as determined by intravital microscopy. IL-1α promotes accumulation of macrophages and neutrophils in inflamed tissue *in-vivo*. Furthermore, IL-1α on monocytes stimulates their homing at sites of vascular injury. A variety of stimuli such as free fatty acids or oxalate crystals induce IL-1α surface expression and release by monocytes, which then mediates their adhesion to the endothelium via IL-1 receptor-1. Besides, IL-1α promotes expression of the vascular cell adhesion molecule-1 (VCAM-1) on endothelial cells thereby fostering the adhesion of circulating leukocytes. IL-1α induces inflammatory injury after experimental AMI and abrogation of IL-1α prevents the development of CKD in oxalate or adenine-fed mice.

Conclusions

IL-1α represents a key mediator of leukocyte-endothelial adhesion and inflammation in cardiorenal diseases. Inhibition of IL-1α may serve as a novel anti-inflammatory treatment strategy.

Introduction

Cardiovascular diseases (CVD) and chronic kidney disease (CKD) are highly prevalent in Western populations and recent reports indicate that their global prevalence is steadily increasing[1]. Both disease entities are associated with high disease-related morbidity and mortality rendering both, CVD and CKD, global public health problems. Particularly, patients after acute myocardial infarction (AMI) show substantially higher mortality compared to the general population[2]. Moreover, CKD accounts for a dramatically reduced life-expectancy mainly due to CVD. Therefore, CKD represents one of the strongest CV risk factors[3]. As compared to subjects without CKD, CV mortality in CKD patients is increased by 4-1000-fold[4]. Notably, CKD is not only a risk factor for CVD, CVD is also associated with the development of kidney dysfunction and its progression, which is referred to as cardiorenal syndrome[5]. The pathophysiological mechanisms leading to CVD in CKD patients are complex and yet only incompletely understood. However, it is commonly accepted that (sterile) systemic inflammation represents a key driver of CVD in the general population[6] and, particularly, in CKD patients[7].

A plethora of studies has documented that despite maximum intensity lipid-lowering therapy a substantial inflammatory residual risk persists[8]. Accordingly, the plasma levels of pro-inflammatory cytokines such as high-sensitivity C-reactive protein (hsCRP) and interleukin-6 (IL-6) are associated with CV events in secondary but also in primary prevention[9-11]. Specific anti-inflammatory treatments such as the inhibition of interleukin-1β by canakinumab or treatment with colchicine have emerged as novel therapeutic strategies, which reduce CV events in patients with prevalent CVD receiving state-of-the-art therapy (i.e. lipid-lowering therapy, antiplatelet agents)[12, 13].

Inflammation can be mediated by activation of the innate immune system by endogenous agents such as modified lipoproteins[7, 14, 15]. This leads to a systemic pro-inflammatory response with the release of cytokines by innate immune effector cells such as monocytes and macrophages. Thereby, cytokines of the IL-1 superfamily play a particularly important role[16]. IL-1β, processed by the NOD-like receptor protein-3 (NLRP3) inflammasome,

has been shown to trigger the development of atherosclerosis[17, 18]. Recently, we have shown that apolipoprotein-C3 – a component of triglyceride-rich lipoprotein – elicits alternative NLRP3 inflammasome activation in human monocytes leading to vascular and kidney injury *in vivo*[14]. While IL-1β in CVD has been extensively studied, the role of IL-1α in the development of CVD remains poorly understood. IL-1α differs from IL-1β in several aspects: In contrast to IL-1β, the precursor form of IL-1α is also biologically active. Pro-IL-1α can be detected within the cell, where it may serve as a transcription factor, but it is also expressed on the surface of the cells[19]. There, it serves as a danger signal for neighboring and circulating cells. Accordingly, IL-1α is considered a key alarmin. Due to its expression on the cell surface, IL-1α is suggested to play an important role in cell-cell contact. Free fatty acids were shown to induce the release of IL-1α from macrophages and deficiency in IL-1α reduces atherosclerotic lesion formation in the murine system[20].

The adhesion of leukocytes such as monocytes to the endothelium and their transmigration into the subendothelial layer represents a crucial first step in the pathogenesis of atherosclerotic CVD[21]. This is mediated by cell adhesion molecules expressed on the surface of endothelial cells. Upon stimulation of the endothelium by e.g. tumor necrosis factor-α (TNF-α), endothelial cells express vascular cell adhesion molecule-1 (VCAM-1), which mediates firm adhesion of circulating monocytes. In the subendothelial layer, these monocytes differentiate into tissue macrophages and acquire lipoproteins such as oxidized LDL (oxLDL) and finally become foam cells[22].

The aim of the present study was to explore the role of IL-1α as a mediator of leukocyte-endothelial adhesion and inflammation in cardiorenal diseases. We tested the relevance of IL-1α-induced leukocyte-endothelial adhesion in several animal models of CV and kidney injury. Furthermore, in a clinical trial we quantified the expression of IL-1α on the surface of monocytes from patients with AMI or CKD, and determined its association with CV events in an explorative clinical study.

Methods

Clinical trial

Patients with AMI (i.e. Non-ST segment elevation myocardial infarction [NSTEMI] or ST-segment elevation myocardial infarction [STEMI]) were recruited at the cardiac intensive care unit of the Saarland University Hospital, Homburg/Saar, Germany. Blood was drawn within 24 hours after coronary angiography. Patients with stable CKD were recruited at our nephrological outpatient clinic or at our dialysis unit, respectively. Healthy subjects were recruited from the employees of the Saarland University Hospital. Only healthy subjects without prevalent CVD or CKD, diabetes, and regular medication were included. After discharge, patients with AMI were followed for a median of 1,478 (IQR: 1,067) days. The combined atherosclerotic CVD (ASCVD) endpoint was defined as the composite of recurrent AMI, hospitalization for unstable angina, coronary angiography with revascularization, stroke, and all-cause mortality. All participants gave their written consent and the study was approved by the local Ethics committee (155/13).

Monocyte isolation and stimulation

EDTA blood samples were immediately processed. Peripheral blood mononuclear cells (PBMCs) were isolated by Ficoll gradient centrifugation. For cell stimulation, $1x10^6$ PBMCs were seeded in 96 well plates in RPMI Glutamax supplemented with 10 % fetal bovine serum, penicillin/streptomycin, and 10 mM HEPES. After one hour, non-adherent cells were removed by washing to enrich monocytes and the medium was changed to RPMI Glutamax supplemented with penicillin/streptomycin, and 10 mM HEPES. Cells were then stimulated with ultrapure lipopolysaccharide (LPS, Invivogen, 3 hours, 100 ng/mL) and afterwards with ATP (Invivogen, 5 mM, 1 hour) or Alum (Invivogen, 200 µg/mL, 3 hours). Supernatants were collected for IL-1α ELISA measurements.

Analysis of IL-1α surface expression by flow cytometry

$1x10^6$ PBMCs were stained with Anti-CD14-PE (Beckton Dickinson), Anti-CD16-APC (BioLegend), and Anti-IL-1α-FITC (eBioscience) antibodies and analyzed using the BD FACS Canto II. The gating strategy is shown in **Supplemental Figure 1A**. Mean fluorescence intensity (MFI) of IL-1α-FITC was determined in the populations of $CD14^{-}CD16^{+}$, $CD14^{+}CD16^{+}$, and $CD14^{+}CD16^{-}$ monocytes. As a control, mouse IgG1 kappa isotype control (P3.6.2.8.1), FITC (eBioscience) was used (**Supplemental Figure 1B**). Analyses were performed using the software FlowJo 10.5.3 (LLC).

Quantitative real-time PCR

Freshly isolated human PBMCs were lysed in Trizol (Invitrogen). RNA extraction was performed using the methanol/chloroform method. A total of 1 µg RNA was reverse transcribed into cDNA (DyNAmo cDNA synthesis kit, ThermoFisher, #F470L). Afterwards, quantitative real-time PCR was performed using the SYBR Green Maxima kit (ThermoScientific, #FERK0253) by using the Mx3000P Real-Time PCR system (Stratagene). The following primers were used: human *IL1A* forwards, 5'-GACGCACTTGTAGCCACGTA-3' and reverse, 5'-TGGCAGCTTAAGCCTGAGTC-3'; human HPRT1 forward, 5'-AGGACTGAACGTCTTGCTCG-3' and reverse, 5'-GAGCACACAGAGGGCTACAA-3'.

IL-1α ELISA

IL-1α concentrations in cell culture supernatants were determined using a commercially available ELISA kit according to the manufacturer's protocol (R&D system, Human-IL-1α/IL-1F1 Duoset, #DY200).

Animal experiments

Il1a$^{-/-}$ mice und *Il1b*$^{-/-}$ mice were provided by Manfred Kopf (ETHZ Zürich, Switzerland) [20]. Corresponding C57/Bl6 wildtype mice were breeded in our local animal facility. All mice were housed in individual cages and fed a standard chow diet unless otherwise indicated. Animals

were used for the experiments at an age of 8-12 weeks. All animal experiments were approved by the Veterinary Office of the Saarland.

Dorsal skinfold chamber

Murine dorsal skinfold chamber model was performed as described previously[23]. Briefly, mice were anesthetized and two symmetrical titanium frames were implanted on the extended dorsal skinfold of the animals, so that they sandwiched the double layer of the skin. Next, one layer of the skin was completely removed in a circular area of 15 mm in diameter. The remaining layers consisting of epidermis, subcutaneous tissue and striated skin muscle were covered with a glass coverslip.

LPS-induced striated skin muscle inflammation

The chamber tissue of wildtype, *Il1b*$^{-/-}$ and *Il1a*$^{-/-}$ mice was topically exposed to 10 µg/mL LPS for 0.5 hour to induce a local inflammation as described previously[23]. Briefly, mice were immobilized on a Plexiglas stage and the dorsal skinfold chamber was attached to the microscopic stage. After retrobulbary i.v. injection of 0.05 mL 5% FITC-dextran 150,000 for contrast enhancement by staining of blood plasma and 0.05 mL 0.1% rhodamine 6G for staining of leukocytes, intravital epi-illumination fluorescence microscopy was performed. The leukocyte-endothelial cell interaction, blood vessel diameter and macromolecular leakage was determined at baseline conditions (19 hours before topical exposure of the chamber tissue to LPS) as well as 0.5 hour, 3 hours and 24 hours after LPS treatment.

Peritoneal inflammation model

Wildtype and *Il1a*$^{-/-}$ mice were intraperitoneally injected with 500 µL of sterile PBS or Zymosan (200 µg/mL). After six hours, the peritoneal cavity was flushed with 5 mL PBS containing 2 mM EDTA and the exudate was collected. After FC blocking, peritoneal cells were stained with APC-Ly6C (BioLegend, clone HK1.4) and PE-Ly6G (BioLegend, clone 1A8) antibodies and quantified by flow cytometry.

Isolation of murine spleen monocytes and PKH67 labeling

Monocytes were isolated from wildtype and *Il1a*$^{-/-}$ mice. A single cell suspension of spleen cells was prepared by using a Spleen Dissocation Kit, mouse (Miltenyi Biotec, #130-095-926). CD11b^{+} spleen monocytes were isolated using MACS sorting (CD11b microbeads, Miltenyi Biotec, #130-049-601). The purity of the cells was determined by flow cytometry. The murine CD11b^{+} monocytes were fluorescently stained using a fluorescence PKH67 labeling kit (Sigma Aldrich, #MINI67-1KT) and immediately used for transplantation into mice subjected to carotid injury.

Carotid injury model

Murine carotid injury model was performed as described[14]. Briefly, wildtype or *Il1a*$^{-/-}$ mice were anaesthetized using isoflurane. The left common carotid artery was injured using a bipolar microregulator by applying an electric current of 2 Watt on a total length of 4 mm. Four hours after carotid injury, mice were transplanted with 1x10^{6} PKH67-labeled CD11b^{+} splenic monocytes obtained from wildtype and *Il1a*$^{-/-}$ mice. 18 hours later, the left common carotid artery was removed and digested in a buffer containing collagenase I, hyaluronidase, collagenase XI and DNase 1 for one hour at 37 °C under gentle agitation. Afterwards, cells were filtered through 70 µM cell strainers and quantified by flow cytometry.

Ligation of the left anterior descending (LAD) coronary artery in mice

Ligation of the LAD was performed as a model of AMI. Mice were anesthetized with ketamine (100 mg/kg)/xylazine (10 mg/kg) and caprofen was used for analgesia. After intubation, mice were ventilated with a stroke volume of 200 µl and a respiration rate of 120 strokes per minute. The chest was opened via the fourth intercostal space at the left upper sternal border through a small incision and AMI was induced by LAD ligation. Control mice underwent sham operation, during which the pericardium was opened. Three days after surgery, mice were anesthetized and sacrificed by cervical dislocation. Hearts were removed for histological analyses.

Oxalate and adenine diet in mice

Mice were subjected to an oxalate diet containing sodium oxalate (50 mmol/kg) and low calcium (Sniff). As a control, mice were subjected to a low calcium diet without sodium oxalate (Sniff). Moreover, mice were subjected to an adenine diet (0.2 %, Altromin) to induce kidney damage. Control mice were fed with a normal chow diet (Altromin). After 2 weeks, mice were euthanized and kidneys were collected for histology. Serum creatinine and urea were determined using a clinical chemistry multianalyzer (BeckmanCoulter AU480).

Histology

Hematoxyline/eosine (HE) and Sirius Red stainings were analyzed using a Zeiss Axio Imager 2 and the software ZEN. Ly6G (eBioscience, #14-5931), F4/80 (Invitrogen, #14-4801-82) and IL-1α (Cusabio, #CSB-PA009537) expression was analyzed using immunofluorescence microscopy. The Ly6G-, F4/80-, and Il-1α-positive areas were quantified using Image J.

Culture of human aortic endothelial cells (HAECs)

HAECs were obtained from Clonetics® and cultured in Endothelial Cell Growth Medium-2 (Clonetics®, Lonza) supplemented with 10 % Fetal Bovine Serum (FBS, Gibco, Invitrogen). Before the experiments, cells were starved in Endothelial Basal Medium (Lonza) with 0.5 % FBS overnight. HAECs were used within passage 4 to 6.

Culture of murine aortic endothelial cells (MAECs)

MAECs were purchased from CellBiologics. They were culture in Endothelial Cell Medium (CellBiologics, #M1168) supplemented with Endothelial Cell Medium Supplement Kit (CellBiologcs, #M1168-KIT). Before the experiments, cells were starved overnight in Endothelial Cell Medium without supplements. MAECs were used within passage 4 to 6.

Stimulation of human or murine PBMCs

PBMCs were isolated from whole blood using Ficoll gradient centrifugation. PBMCs were stimulated with LPS (Invivogen, 18 hours, 100 ng/mL), TNF-a (R&D systems, 5 ng/mL), LPS + oleic acid (LPS 100 ng/mL for 18 hours, 100 µM oleic acid for 4 hours) or LPS + oxalate (LPS 100 ng/mL for 18 hours, 100 µg/mL for 4 hours). Oleic acid was dissolved in Cremaphor as described[20]. Where indicated cells were incubated in the presence of Z-Leu-Leu-CHO (Enzo Lifescience, #BMP-PI116, 1.2 µM), E-64-d (Enzo Lifescience, #BML-PI107, 50 µg/mL), EGTA (Sigma Aldrich, 20 mM), or BAPTA-AM (Sigma Aldrich, #BCBW1114V, 10 µM).

Leukocyte-endothelial adhesion assay

To assess leukocyte-endothelial adhesion, 10,000 HAECs or MAECs were seeded in fibronectin-(HAEC) or gelatin-coated (MAEC, PELOBiotech, #6950) eight-well chamber slides and incubated with DiI-labeled human or murine PBMCs for 18 hours. Non-adherent cells were removed by washing and endothelial cells were counterstained with DAPI mounting medium (Vectashild). Adherent PBMCs were counted in four random power fields using Axio Imager.M2. Where indicated, PBMCs were preincubated (1 hour) with an Anti-IL-1α blocking antibody (Invivogen, #mabg-hil1a, 1 µg/mL) and HAECs with an Anti-IL1R1 blocking antibody (R&D systems, #AB-269-NA, 10 µg/mL or respective isotype control.

Western blot analyses

Protein expression was determined by Western blot analysis. Cells were lysed in lysis buffer containing 50 mmol/l Tris pH 7.5, 150 mmol/L NaCl, 1 mmol/L EDTA, 0.5 % NP-40 supplemented with protease and phosphatase inhibitors. 30 µg of protein from HAECs were loaded per lane, resolved by 10 % SDS-PAGE, transferred to a PVDF membrane (Millipore, Billerica, MA, USA) by semidry transfer. The following antibodies and dilutions were used: Goat anti-human VCAM-1 (R&D systems, Abingdon, UK, polyclonal) 1:2,000, Mouse-anti human glycerinaldehyde-3-phosphate-dehydrogenase (Millipore, clone: 6C5) 1:20,000 as loading control. Protein in cell culture supernatants from PBMCs was precipitated using trichloroacetic (TCA) acid. To 500 µL supernatant 500 µL TCA 20 % were added. After 30

minutes of incubation at 4 °C, samples were centrifuged (12,000 g, 15 minutes, 4 °C) and washed three times. Afterwards, 1 mL acetone was added and samples were centrifuged again (12,000 g, 5 minutes, 4 °C), supernatant was removed and the pellet resuspended in 50 µL sample buffer. Proteins were resolved by 10-15 % SDS-PAGE and transferred onto a nitrocellulose membrane (0.2 µm, GE Healthcare life science). The following antibodies were used: Rabbit-anti human IL-1α (Abcam, #ab9614) 1:1,000, and Anti-human β-Actin antibody (Santa Cruz biotechnology, #sc-47778) 1:2,000 as loading control.

Statistical analyses

Statistical analyses were carried out using GraphPad Prism 5, and SPSS 25. Unless otherwise stated, results are presented as mean±SEM. Statistical differences were examined using One-Way ANOVA followed by Dunnett's post-hoc test to adjust for multiple comparisons for analyses of >2 groups and with Student's T test for two groups. All measurements were taken from distinct samples. In the explorative clinical study of patients with AMI, IL-1α FITC MFI was dichotomized at median. Association between IL-1α FITC MFI and the combined ASCVD endpoint during follow-up was assessed by Cox regression analyses adjusted for age, sex, body mass index (BMI), diabetes, arterial hypertension, smoking, and hsCRP. A two-sided *P* value <0.05 was considered significant.

Results

IL-1α is expressed on monocytes from patients with AMI and in patients with CKD

IL-1α expression was quantitated on the surface of distinct monocyte subtypes (i.e. $CD14^+CD16^-$, $CD14^-CD16^+$, and $CD14^+CD16^+$ in a clinical study including 36 healthy subjects, 58 patients with stable CKD, and 71 patients with AMI (**Figure 1A**). Baseline characteristics are shown in **Supplemental Table 1**. Compared to healthy subjects, IL-1α surface expression on all three monocyte subclasses was significantly higher in AMI patients (i.e. NSTEMI or STEMI) and CKD patients (**Figure 1B-D**, **Supplemental Figure 1A+B**). The expression of *Il1a* mRNA was significantly higher in monocytes from patients with AMI or CKD alike in comparison to cells from healthy subjects (**Figure 1E**). Upon stimulation with known activators of IL-1α, monocytes from patients with AMI and CKD released significantly greater amounts of IL-1α into the cell culture supernatants (**Figure 1F-G**).

IL-1α expression on the surface of monocytes associates with CV events

To prove the clinical relevance, we assessed the association between IL-1α surface expression on monocytes quantified at the time of AMI with ASCVD events after a median follow-up of 4 years. Higher IL-1α surface expression on $CD14^+CD16^-$ and $CD14^+CD16^+$ monocytes was associated with a significantly higher risk for ASCVD events (HR 8.78, 95% CI: 2.54-30.33 and HR 3.43, 95% CI: 1.17-10.11). This association was independent of potential confounding variables including hsCRP (**Figure 2A+C**, **Supplemental Table 2**). IL-1α surface expression on $CD14^-CD16^+$ monocytes was not significantly associated with ASCVD events (HR: 2.17, 95% CI: 0.81-5.85, **Figure 2B**, **Supplemental Table 2**).

IL-1α but not IL-1β mediates leukocyte-endothelial adhesion

Since the pro-form of IL-1α is expressed on the surface of leukocytes and is biologically active, we tested the role of IL-1α as a mediator of leukocyte-endothelial adhesion. For this purpose, we used the dorsal skinfold chamber model in combination with the intravital fluorescence

(**Figure 3A**). At baseline, leukocyte adhesion did not differ between wildtype, *Il1a*$^{-/-}$, and *Il1b*$^{-/-}$ mice (**Figure 3B+F**). However, topical application of LPS induced rapid leukocyte-endothelial adhesion, which was significantly attenuated in *Il1a*$^{-/-}$ mice during the entire observation period of 24 hours when compared to wildtype mice. In contrast, leukocyte adhesion was not altered in *Il1b*$^{-/-}$ mice. The number of rolling leukocytes, macromolecular leakage and the blood vessel diameter did not differ between the three groups (**Figure 3C-F**). These findings point to a pivotal role of IL-1α in mediating leukocyte-endothelial adhesion. Therefore, the following experiments focused on IL-1α.

IL-1α mediates leukocyte tissue infiltration upon inflammation

Next, we tested the ability of IL-1α to elicit leukocyte infiltration into inflamed tissues. The application of LPS using the dorsal skinfold chamber model (**Figure 4A**) led to a strong infiltration of the skin tissue with F4/80^{+} macrophages and Ly6G^{+} neutrophils (**Figure 4B+C**). As compared to wildtype mice, the number of skin-infiltrating macrophages and neutrophils was significantly lower in *Il1a*$^{-/-}$ mice. To confirm these findings, we performed a peritoneal inflammation model and induced sterile peritonitis by intraperitoneal injection of zymosan (**Figure 4D**). After six hours, the number of peritoneal monocytes and neutrophils was quantified using flow cytometry. At baseline, the peritoneal monocyte and neutrophil count did not differ between wildtype and *Il1a*$^{-/-}$ mice (**Figure 4E-F**). However, after application of zymosan, knockout of *Il1a* significantly reduced the number of peritoneal monocytes and neutrophils. To underscore the relevance of these findings in CVD, we assessed the effect of IL-1α on the homing of leukocytes in the area of vascular injury. For this purpose, wildtype mice and *Il1a*$^{-/-}$ mice transplanted with PKH67-labeled monocytes from wildtype or *Il1a*$^{-/-}$ mice underwent perivascular injury of the carotid artery (**Figure 4G**), a model for vascular regeneration. Eighteen hours after injury, carotid arteries were collected, digested and the number of infiltrating PKH67^{+} monocytes was quantified. The number of PKH67^{+} cells in the carotid artery of wildtype mice receiving *Il1a*$^{-/-}$ monocytes was significantly lower as compared to *Il1a*$^{-/-}$ mice transplanted with monocytes from wildtype mice (**Figure 4H**). This indicates that

leukocyte-endothelial interaction is primarily mediated by IL-1α on monocytes but not on endothelial cells.

Endogenous mediators induce IL-1α expression in human monocytes

It has been recently shown that free fatty acids, whose concentrations are elevated in patients with CKD or AMI, induce the expression and release of IL-1α in murine macrophages[20]. In addition, we tested crystals as another activator of IL-1α[24]. The experiments show that oleic acid (OA) and oxalate (Ox) crystals increased pro-IL-1α expression in the cell lysate and mature IL-1α released into the supernatant of human monocytes (**Figure 5A+B**). Importantly, both, OA and Ox also increased the expression of IL-1α on the surface of monocytes (**Figure 5C**). In contrast, we found that these stimuli did not affect the release of IL-1α from HAECs (data not shown). Recently, it has been shown that calcium-dependent activation of the protease calpain plays a central role in processing pro-IL-1α into its mature form[20]. Therefore, we stimulated monocytes again in the presence of calcium chelators (BAPTA-AM or EGTA) or calpain inhibitors (Z-Leu-Leu-CHO or E-64-d) and quantified IL-1α release (**Figure 5D**). All four inhibitors significantly reduced IL-1α in response to LPS+Ox or LPS+OA.

IL-1α induces the expression of VCAM-1 on aortic endothelial cells

Since *Il1a*$^{-/-}$ strongly reduced leukocyte-endothelial adhesion *in vivo*, we tested the effect of IL-1α on the adhesion of monocytes to HAECs *in vitro* and the individual contribution of IL-1α and its receptor IL-1R1 (**Figure 6A**). Stimulation of monocytes with LPS+OA or LPS+Ox, which increases IL-1α surface expression, promoted adhesion of these cells to a monolayer of HAECs. Importantly, this was prevented by either incubating the monocytes with an anti-IL-1α blocking antibody or with an anti-IL-1R1 blocking antibody. Notably, neither anti-IL-1α nor anti-IL-1R1 blockade had any effect on baseline or TNF-α-stimulated monocyte-endothelial adhesion. These findings indicate that IL-1α and its receptor IL-1R1 play a pivotal role in leukocyte-endothelial adhesion. Incubating HAECs with increasing concentrations of IL-1α

significantly increased the expression of the cell adhesion molecule VCAM-1 (**Figure 6B**). The incubation of the HAECs with LPS+OA or LPS+Ox did not affect endothelial VCAM-1 expression (**Figure 6C**). This indicates that IL-1α induces increased expression and release of IL-1α by monocytes, which provokes endothelial VCAM-1 expression and subsequent adhesion of these monocytes to the endothelium. Using murine MAECs incubated with monocytes from either wildtype or *Il1a*$^{-/-}$ mice, we confirmed that the absence of *Il1a*$^{-/-}$ on monocytes reduces the adhesion of monocytes to the endothelium (**Figure 6D**).

IL-1α promotes leukocyte accumulation after acute myocardial infarction

To confirm the *in vivo* relevance of these findings, we subjected wildtype and *Il1a*$^{-/-}$ mice to permanent ligation of the LAD coronary artery, as an established model of AMI (**Figure 7A**). Interestingly, we observed that IL-1α was highly expressed in the infarction area three days after LAD ligation. In contrast, no IL-1α was detectable in the uninjured area or in mice undergoing sham surgery (**Figure 7B**). To test whether IL-1α mediates myocardial accumulation of leukocytes after AMI, wildtype and *Il1a*$^{-/-}$ mice were subjected to LAD ligation or sham procedure. IL-1α deficiency reduced inflammation after AMI (**Figure 7C**) and the number of myocardium-infiltrating F4/80^{+} macrophages and Ly6G^{+} neutrophils (**Figure 7D+E**, **Supplemental Figure 2A+B**).

IL-1α promotes kidney injury

Next, we assessed the contribution of IL-1α to experimental kidney injury. Since we found that Ox induces the release of IL-1α from human monocytes *in vitro*, mice were subjected to an oxalate diet for two weeks (**Figure 8A**). Oxalate feeding increased the creatinine and urea serum levels in wildtype mice (**Figure 8B+C**). Creatinine and urea concentrations were significantly lower in *Il1a*$^{-/-}$ mice on the oxalate diet. The oxalate diet promoted kidney fibrosis in wildtype mice, which was significantly attenuated in *Il1a*$^{-/-}$ mice (**Figure 8D**). We found that IL-1α-deficiency strongly attenuated the accumulation of macrophages and neutrophils within

the injured kidneys (**Figure 8E-F**). To prove that the effect of IL-1α on kidney injury was not restricted to the oxalate mouse model, CKD was induced by administration of an adenine diet (**Supplemental figure 3A**). While serum creatinine and urea levels did not differ between wildtype and *Il1a*$^{-/-}$ mice on adenine diet, kidney fibrosis was significantly attenuated in *Il1a*$^{-/-}$ mice (**Supplemental figure 3B-D**). The numbers of kidney-infiltrating macrophages and neutrophils were significantly reduced in the absence of IL-1α in comparison to wildtype mice.

Discussion

Here, we identified IL-1α as a central regulator of inflammation in CVD and kidney diseases. IL-1α is released from human monocytes by endogenous stimuli such as oleic acid and oxalate and expressed on their surface. It activates endothelial cells to express cell adhesion molecules and, thereby, promotes leukocyte-endothelial adhesion, but it also serves as a cell adhesion molecule as summarized in **Supplemental Figure 4**. Abrogation of IL-1α reduces myocardial inflammation after AMI and ameliorates experimental CKD. IL-1α is expressed on the surface of monocytes from patients with AMI and CKD, and its expression is associated with future CV events.

IL-1α is a constitutively expressed cytokine in many different cell types[19]. We found that oxalate and oleic acid increase the expression of IL-1α on the surface of monocytes and its release. IL-1α is expressed within the injured myocardium, where it serves as a danger signal. Indeed, it has been documented that IL-1α represents a key player required for the sterile inflammation in response to necrotic cells[25], which is particularly characterized by the accumulation of neutrophils[26]. Our data show that IL-1α deficiency reduced the number of accumulating neutrophils after myocardial or kidney injury. Apoptotic vascular smooth muscle cell express IL-1α[27] and necrotic myocardial cells release IL-1α, which then promotes fibroblast activation[28]. Besides, apoptotic bodies and neutrophil extracellular traps induce endothelial inflammation via IL-1α-dependent pathways[29, 30] and also platelets carry IL-1α, which induces the expression of cell adhesion on the cerebral vessels driving cerebrovascular inflammation and damage[31, 32].

Intravital microscopy revealed that IL-1α but not IL-1β is involved in the leukocyte-endothelial adhesion. Although both cytokines belong to the IL-1 superfamily, they show important differences. While the NLRP3 inflammasome mediates cleavage of pro-IL-1α into its secreted mature form, pathways independent of the caspase-1 catalytic activity have been described for IL-1α[24]. Therefore, several inflammasome activators such as Alum or ATP also induce IL-1α release, while, for instance, free fatty acids promote the maturation of IL-1α but

not of IL-1β[20]. Mitochondrial uncoupling and subsequent cellular calcium influx activate the calcium-dependent protease calpain, which induces cleavage of pro-IL-1α into its mature form[20]. Another key difference between IL-1β and IL-1α is the biological activity of the precursor forms. While pro-IL-1β requires caspase-1-dependent cleavage to confer its proinflammatory activity, the IL-1α precursor is equally active in inducing a pro-inflammatory response[33]. Pro-IL-1α can be released from stressed cells but is also expressed on the cell surface. Interestingly, we found that the expression of pro-IL-1α was significantly higher on the surface of monocytes from patients with AMI or CKD as compared to healthy subjects. Since antibody blocking of IL-1α on monocytes reduced the adhesion of monocytes to endothelial cells and *Il1a*$^{-/-}$ monocytes showed reduced homing at sites of vascular injury, we speculate that IL-1α itself serves as a cell adhesion molecule. Genetic IL-1α deficiency prevented the adhesion of leukocytes to the endothelium already after 30 minutes in the dorsal skinfold chamber experiments. This time is too short to be mediated by *de novo* endothelial expression of cell adhesion molecules such as VCAM-1, which usually requires at least three hours. At later time points, IL-1α induces endothelial VCAM-1 expression and then mediates firm endothelial adhesion of leukocytes.

Our study documented that IL-1α regulates tissue accumulation of neutrophils and macrophages, and thereby inflammatory injury in cardiorenal diseases. It has been documented that leukocyte adhesion plays a pivotal role in mediating CV and kidney damage[6, 21]. Therefore, IL-1α might play an important role in the development of CVD and CKD. Indeed, it has been shown that deficiency of IL-1α in bone-marrow-derived cells significantly reduced atherosclerotic lesions formation in experimental atherosclerosis, while *Il1b*$^{-/-}$ had no significant effect[20]. Neutralization of IL-1α reduced outward remodeling during early atherogenesis[34]. Moreover, IL-1α released by necrotic cardiomyocytes activates cardiac fibroblasts and drives a systemic proinflammatory milieu after AMI[35] and fibroblast-specific deletion of IL-1R1 attenuated adverse cardiac remodeling after AMI[36].

These findings highlight IL-1α as an important mediator of inflammation in AMI and CKD. Since IL-1α surface expression on monocytes is associated with a higher risk for CV events, we propose that it is worthwhile to test IL-1α as a therapeutic target at least during the early stages after AMI and possibly also in CKD. Anti-inflammatory treatment strategies have recently emerged as novel therapeutic approaches in the treatment of CVD as evidenced by the CANTOS and COLCOT trials[12, 13]. However, it has been shown that other cytokines such as IL-6 or IL-18 remain elevated after specific inhibition of IL-1β, and are still associated with persistent CV risk[37]. Since IL-1α represents a key regulator of inflammation not only inducing IL-R1-dependent effects but also the release of other proinflammatory cytokines, therapeutic inhibition of IL-1α might provide a complimentary anti-inflammatory treatment strategy. A recombinant human IL-1α-targeting antibody MABp1 has been evaluated in patients with cancer. MABp1 treatment in patients with refractory cancers was well-tolerated and disease control was observed in a phase 1 clinical trial[38]. In a phase 3 clinical trial comprising patients with advanced colorectal cancer, MABp1 treatment was associated with better clinical performance[39]. Interestingly, rilonacept, an IL-1α and IL-1β trap, led to rapid resolution of recurrent pericarditis and lower incidence of relapses as compared to placebo treatment[40]. In addition, a recent experimental study indicates that antibody-mediated inhibition of IL-1α reduces brain damage and neurological deficit in experimental stroke[41]. Specific clinical trials testing the effects of IL-1α inhibition in the setting of cardiorenal injury have not yet been performed.

Our study has limitations. Isolation of monocytes from 165 subjects was an extensive procedure. Therefore, the size of the clinical cohort is moderate and only included patients of Caucasian ancestry. However, in this cohort, we observed a significant increase of IL-1α surface expression on monocytes from patients with AMI as well as patients with CKD. Moreover, in AMI patients, higher IL-1α expression was associated with a higher risk for CV events. This underlines the clinical importance of IL-1α as a mediator of inflammation in CVD. The experimental studies including seven different mouse models focused on inflammation,

which occurs early in the course of AMI and CKD. Therefore, the effects of IL-1α in later disease stages after AMI and in CKD will be the subject of future studies.

In summary, our results highlight IL-1α as a central regulator of inflammation in CVD and CKD. IL-1α mediates myocardial inflammation after AMI and promotes CKD. Moreover, in a translational study, IL-1α expression on monocytes associates with adverse outcomes in patients with AMI. The data suggest that inhibition of IL-1α might represent a promising anti-inflammatory treatment strategy.

Acknowledgments

Funded by the Deutsche Forschungsgemeinschaft (DFG, German Research Foundation) – SFB TRR 219 – Project-ID 322900939. PB is also supported by the German Research Foundation (DFG; SFB/TRR57, BO3755/3-1, BO3755/9-1, BO3755/13-1) and the German Federal Ministries of Education and Research (BMBF: STOP-FSGS-01GM1901A).

Conflict of interests

The authors do not declare any competing interests.

References

1. Disease GBD, Injury I, Prevalence C. Global, regional, and national incidence, prevalence, and years lived with disability for 310 diseases and injuries, 1990-2015: a systematic analysis for the Global Burden of Disease Study 2015. *Lancet.* 2016;388:1545-1602.

2. Bonaca MP, Bhatt DL, Cohen M, Steg PG, Storey RF, Jensen EC, Magnani G, Bansilal S, Fish MP, Im K, Bengtsson O, Oude Ophuis T, Budaj A, Theroux P, Ruda M, Hamm C, Goto S, Spinar J, Nicolau JC, Kiss RG, Murphy SA, Wiviott SD, Held P, Braunwald E, Sabatine MS, Committee P-TS, Investigators. Long-term use of ticagrelor in patients with prior myocardial infarction. *N Engl J Med.* 2015;372:1791-1800.

3. Chronic Kidney Disease Prognosis C, Matsushita K, van der Velde M, Astor BC, Woodward M, Levey AS, de Jong PE, Coresh J, Gansevoort RT. Association of estimated glomerular filtration rate and albuminuria with all-cause and cardiovascular mortality in general population cohorts: a collaborative meta-analysis. *Lancet.* 2010;375:2073-2081.

4. Go AS, Chertow GM, Fan D, McCulloch CE, Hsu CY. Chronic kidney disease and the risks of death, cardiovascular events, and hospitalization. *N Engl J Med.* 2004;351:1296-1305.

5. Rangaswami J, Bhalla V, Blair JEA, Chang TI, Costa S, Lentine KL, Lerma EV, Mezue K, Molitch M, Mullens W, Ronco C, Tang WHW, McCullough PA, American Heart Association Council on the Kidney in Cardiovascular D, Council on Clinical C. Cardiorenal Syndrome: Classification, Pathophysiology, Diagnosis, and Treatment Strategies: A Scientific Statement From the American Heart Association. *Circulation.* 2019;139:e840-e878.

6. Hansson GK. Inflammation and Atherosclerosis: The End of a Controversy. *Circulation.* 2017;136:1875-1877.

7. Zewinger S, Schumann T, Fliser D, Speer T. Innate immunity in CKD-associated vascular diseases. *Nephrol Dial Transplant.* 2016;31:1813-1821.

8. Pradhan AD, Aday AW, Rose LM, Ridker PM. Residual Inflammatory Risk on Treatment With PCSK9 Inhibition and Statin Therapy. *Circulation.* 2018;138:141-149.

9. Ridker PM, Cannon CP, Morrow D, Rifai N, Rose LM, McCabe CH, Pfeffer MA, Braunwald E, Pravastatin or Atorvastatin E, Infection Therapy-Thrombolysis in Myocardial Infarction I. C-reactive protein levels and outcomes after statin therapy. *N Engl J Med.* 2005;352:20-28.

10. Ridker PM, Hennekens CH, Buring JE, Rifai N. C-reactive protein and other markers of inflammation in the prediction of cardiovascular disease in women. *N Engl J Med.* 2000;342:836-843.

11. Ridker PM, MacFadyen JG, Glynn RJ, Bradwin G, Hasan AA, Rifai N. Comparison of interleukin-6, C-reactive protein, and low-density lipoprotein cholesterol as biomarkers of residual risk in contemporary practice: secondary analyses from the Cardiovascular Inflammation Reduction Trial. *Eur Heart J.* 2020;41:2952-2961.

12. Ridker PM, Everett BM, Thuren T, MacFadyen JG, Chang WH, Ballantyne C, Fonseca F, Nicolau J, Koenig W, Anker SD, Kastelein JJP, Cornel JH, Pais P, Pella D, Genest J, Cifkova R, Lorenzatti A, Forster T, Kobalava Z, Vida-Simiti L, Flather M, Shimokawa H, Ogawa H, Dellborg M, Rossi PRF, Troquay RPT, Libby P, Glynn RJ, Group CT. Antiinflammatory Therapy with Canakinumab for Atherosclerotic Disease. *N Engl J Med.* 2017;377:1119-1131.

13. Tardif JC, Kouz S, Waters DD, Bertrand OF, Diaz R, Maggioni AP, Pinto FJ, Ibrahim R, Gamra H, Kiwan GS, Berry C, Lopez-Sendon J, Ostadal P, Koenig W, Angoulvant D, Gregoire JC, Lavoie MA, Dube MP, Rhainds D, Provencher M, Blondeau L, Orfanos A, L'Allier PL, Guertin MC, Roubille F. Efficacy and Safety of Low-Dose Colchicine after Myocardial Infarction. *N Engl J Med.* 2019.

14. Zewinger S, Reiser J, Jankowski V, Alansary D, Hahm E, Triem S, Klug M, Schunk SJ, Schmit D, Kramann R, Korbel C, Ampofo E, Laschke MW, Selejan SR, Paschen A, Herter T, Schuster S, Silbernagel G, Sester M, Sester U, Assmann G, Bals R, Kostner G, Jahnen-Dechent W, Menger MD, Rohrer L, Marz W, Bohm M, Jankowski J, Kopf M,

Latz E, Niemeyer BA, Fliser D, Laufs U, Speer T. Apolipoprotein C3 induces inflammation and organ damage by alternative inflammasome activation. *Nat Immunol.* 2020;21:30-41.

15. Speer T, Rohrer L, Blyszczuk P, Shroff R, Kuschnerus K, Krankel N, Kania G, Zewinger S, Akhmedov A, Shi Y, Martin T, Perisa D, Winnik S, Muller MF, Sester U, Wernicke G, Jung A, Gutteck U, Eriksson U, Geisel J, Deanfield J, von Eckardstein A, Luscher TF, Fliser D, Bahlmann FH, Landmesser U. Abnormal high-density lipoprotein induces endothelial dysfunction via activation of Toll-like receptor-2. *Immunity.* 2013;38:754-768.

16. Abbate A, Toldo S, Marchetti C, Kron J, Van Tassell BW, Dinarello CA. Interleukin-1 and the Inflammasome as Therapeutic Targets in Cardiovascular Disease. *Circ Res.* 2020;126:1260-1280.

17. Duewell P, Kono H, Rayner KJ, Sirois CM, Vladimer G, Bauernfeind FG, Abela GS, Franchi L, Nunez G, Schnurr M, Espevik T, Lien E, Fitzgerald KA, Rock KL, Moore KJ, Wright SD, Hornung V, Latz E. NLRP3 inflammasomes are required for atherogenesis and activated by cholesterol crystals. *Nature.* 2010;464:1357-1361.

18. Sheedy FJ, Grebe A, Rayner KJ, Kalantari P, Ramkhelawon B, Carpenter SB, Becker CE, Ediriweera HN, Mullick AE, Golenbock DT, Stuart LM, Latz E, Fitzgerald KA, Moore KJ. CD36 coordinates NLRP3 inflammasome activation by facilitating intracellular nucleation of soluble ligands into particulate ligands in sterile inflammation. *Nat Immunol.* 2013;14:812-820.

19. Di Paolo NC, Shayakhmetov DM. Interleukin 1alpha and the inflammatory process. *Nat Immunol.* 2016;17:906-913.

20. Freigang S, Ampenberger F, Weiss A, Kanneganti TD, Iwakura Y, Hersberger M, Kopf M. Fatty acid-induced mitochondrial uncoupling elicits inflammasome-independent IL-1alpha and sterile vascular inflammation in atherosclerosis. *Nat Immunol.* 2013;14:1045-1053.

21. Shi C, Pamer EG. Monocyte recruitment during infection and inflammation. *Nat Rev Immunol.* 2011;11:762-774.

22. Weber C, Zernecke A, Libby P. The multifaceted contributions of leukocyte subsets to atherosclerosis: lessons from mouse models. *Nat Rev Immunol.* 2008;8:802-815.

23. Ampofo E, Rudzitis-Auth J, Dahmke IN, Rossler OG, Thiel G, Montenarh M, Menger MD, Laschke MW. Inhibition of protein kinase CK2 suppresses tumor necrosis factor (TNF)-alpha-induced leukocyte-endothelial cell interaction. *Biochim Biophys Acta.* 2015;1852:2123-2136.

24. Gross O, Yazdi AS, Thomas CJ, Masin M, Heinz LX, Guarda G, Quadroni M, Drexler SK, Tschopp J. Inflammasome activators induce interleukin-1alpha secretion via distinct pathways with differential requirement for the protease function of caspase-1. *Immunity.* 2012;36:388-400.

25. Chen CJ, Kono H, Golenbock D, Reed G, Akira S, Rock KL. Identification of a key pathway required for the sterile inflammatory response triggered by dying cells. *Nat Med.* 2007;13:851-856.

26. Lukens JR, Vogel P, Johnson GR, Kelliher MA, Iwakura Y, Lamkanfi M, Kanneganti TD. RIP1-driven autoinflammation targets IL-1alpha independently of inflammasomes and RIP3. *Nature.* 2013;498:224-227.

27. Clarke MC, Talib S, Figg NL, Bennett MR. Vascular smooth muscle cell apoptosis induces interleukin-1-directed inflammation: effects of hyperlipidemia-mediated inhibition of phagocytosis. *Circ Res.* 2010;106:363-372.

28. Zhang W, Lavine KJ, Epelman S, Evans SA, Weinheimer CJ, Barger PM, Mann DL. Necrotic myocardial cells release damage-associated molecular patterns that provoke fibroblast activation in vitro and trigger myocardial inflammation and fibrosis in vivo. *J Am Heart Assoc.* 2015;4:e001993.

29. Folco EJ, Mawson TL, Vromman A, Bernardes-Souza B, Franck G, Persson O, Nakamura M, Newton G, Luscinskas FW, Libby P. Neutrophil Extracellular Traps Induce Endothelial Cell Activation and Tissue Factor Production Through Interleukin-1alpha and Cathepsin G. *Arterioscler Thromb Vasc Biol.* 2018;38:1901-1912.

30. Berda-Haddad Y, Robert S, Salers P, Zekraoui L, Farnarier C, Dinarello CA, Dignat-George F, Kaplanski G. Sterile inflammation of endothelial cell-derived apoptotic bodies is mediated by interleukin-1alpha. *Proc Natl Acad Sci U S A.* 2011;108:20684-20689.

31. Thornton P, McColl BW, Greenhalgh A, Denes A, Allan SM, Rothwell NJ. Platelet interleukin-1alpha drives cerebrovascular inflammation. *Blood.* 2010;115:3632-3639.

32. Orsini F, Fumagalli S, Csaszar E, Toth K, De Blasio D, Zangari R, Lenart N, Denes A, De Simoni MG. Mannose-Binding Lectin Drives Platelet Inflammatory Phenotype and Vascular Damage After Cerebral Ischemia in Mice via IL (Interleukin)-1alpha. *Arterioscler Thromb Vasc Biol.* 2018;38:2678-2690.

33. Kim B, Lee Y, Kim E, Kwak A, Ryoo S, Bae SH, Azam T, Kim S, Dinarello CA. The Interleukin-1alpha Precursor is Biologically Active and is Likely a Key Alarmin in the IL-1 Family of Cytokines. *Frontiers in immunology.* 2013;4:391.

34. Vromman A, Ruvkun V, Shvartz E, Wojtkiewicz G, Santos Masson G, Tesmenitsky Y, Folco E, Gram H, Nahrendorf M, Swirski FK, Sukhova GK, Libby P. Stage-dependent differential effects of interleukin-1 isoforms on experimental atherosclerosis. *Eur Heart J.* 2019;40:2482-2491.

35. Lugrin J, Parapanov R, Rosenblatt-Velin N, Rignault-Clerc S, Feihl F, Waeber B, Muller O, Vergely C, Zeller M, Tardivel A, Schneider P, Pacher P, Liaudet L. Cutting edge: IL-1alpha is a crucial danger signal triggering acute myocardial inflammation during myocardial infarction. *J Immunol.* 2015;194:499-503.

36. Bageghni SA, Hemmings KE, Yuldasheva NY, Maqbool A, Gamboa-Esteves FO, Humphreys NE, Jackson MS, Denton CP, Francis S, Porter KE, Ainscough JF, Pinteaux E, Drinkhill MJ, Turner NA. Fibroblast-specific deletion of interleukin-1 receptor-1 reduces adverse cardiac remodeling following myocardial infarction. *JCI Insight.* 2019;5.

37. Ridker PM, MacFadyen JG, Thuren T, Libby P. Residual inflammatory risk associated with interleukin-18 and interleukin-6 after successful interleukin-1beta inhibition with canakinumab: further rationale for the development of targeted anti-cytokine therapies for the treatment of atherothrombosis. *Eur Heart J.* 2020;41:2153-2163.

38. Hong DS, Hui D, Bruera E, Janku F, Naing A, Falchook GS, Piha-Paul S, Wheler JJ, Fu S, Tsimberidou AM, Stecher M, Mohanty P, Simard J, Kurzrock R. MABp1, a first-in-class true human antibody targeting interleukin-1alpha in refractory cancers: an open-label, phase 1 dose-escalation and expansion study. *Lancet Oncol.* 2014;15:656-666.

39. Hickish T, Andre T, Wyrwicz L, Saunders M, Sarosiek T, Kocsis J, Nemecek R, Rogowski W, Lesniewski-Kmak K, Petruzelka L, Apte RN, Mohanty P, Stecher M, Simard J, de Gramont A. MABp1 as a novel antibody treatment for advanced colorectal cancer: a randomised, double-blind, placebo-controlled, phase 3 study. *Lancet Oncol.* 2017;18:192-201.

40. Klein AL, Imazio M, Cremer P, Brucato A, Abbate A, Fang F, Insalaco A, LeWinter M, Lewis BS, Lin D, Luis SA, Nicholls SJ, Pano A, Wheeler A, Paolini JF, Investigators R. Phase 3 Trial of Interleukin-1 Trap Rilonacept in Recurrent Pericarditis. *N Engl J Med.* 2020.

41. Liberale L, Bonetti NR, Puspitasari YM, Schwarz L, Akhmedov A, Montecucco F, Ruschitzka F, Beer JH, Luscher TF, Simard J, Libby P, Camici GG. Postischemic Administration of IL-1alpha Neutralizing Antibody Reduces Brain Damage and Neurological Deficit in Experimental Stroke. *Circulation.* 2020;142:187-189.

Figure legends

Figure 1: **IL-1α expression in monocytes from patients with AMI and patients with CKD**

A Outline of the clinical study to assess the expression and the release of IL-1α in monocytes obtained from patients with CKD (N=58), AMI (N=71), and healthy subjects (N=36). **B-D** Mean fluorescence intensity (MFI) of IL-1α-FITC on the surface of $CD14^+CD16^-$, $CD14^-CD16^+$, and $CD14^+CD16^+$ monocytes. **E** *Il1a* mRNA expression in PBMCs. **F-G** Release of IL-1α in the supernatant of monocytes primed with LPS (3 hours, 100 µg/mL) and stimulated with ATP (1 hour, 5 mM) or Alum (3 hours, 200 µg/mL). Statistical comparisons were made to healthy subjects. * $P<0.05$, ** $P<0.01$, *** $P<0.001$, **** $P<0.0001$.

Figure 2: **IL-1α surface expression of monocytes obtained from patients with AMI associates with cardiovascular events**

A-C Association between IL-1α FITC MFI on $CD14^+CD16^-$, $CD14^-CD16^+$, and $CD14^+CD16^+$ monocytes dichotomized at the median with the combined cardiovascular endpoint as determined by Cox regression analyses adjusted for age, sex, body mass index, diabetes, arterial hypertension, smoking, and high sensitivity C-reactive protein.

Figure 3: **IL-1α mediates leukocyte-endothelial adhesion in the dorsal skinfold chamber as determined by intravital microscopy**

A Outline of the experiments using the dorsal skinfold chamber in wildtype (WT), *Il1a*$^{-/-}$, and *Il1b*$^{-/-}$ mice. IVM, intravital microscopy. **B** Number of adhering and **C** rolling rhodamine-labeled leukocytes after local LPS application (N=6-8 per group). **D** Macromolecular leakage of FITC-dextran as determined by IVM (N=6-8 per group). **E** Vessel diameter after LPS treatment (N=6-8 per group). **F** Representative intravital microscopic images of collecting venules in dorsal skinfold chambers.

Figure 4: **IL-1α mediates tissue infiltration with macrophages and neutrophils**

A Outline of the murine LPS skin model. **B-C** Infiltration of the skin with F4/80$^+$ macrophages and Ly6G$^+$ neutrophils after local LPS challenge in wildtype (WT) and *Il1a*$^{-/-}$ mice (N=5 per group). **D** Outline of the peritoneal inflammation model. **E-F** Monocytes and neutrophils in the peritoneal fluid of WT and *Il1a*$^{-/-}$ mice six hours after intraperitoneal PBS or Zymosan (200 µg/mL) application as determined by flow cytometry (N=3-4 per group). **G** Outline of the carotid injury model. **H** Homing of PKH67-stained CD11b$^+$ monocytes from WT and *Il1a*$^{-/-}$ mice in the carotid artery of WT and *Il1a*$^{-/-}$ mice 18 hours after perivascular injury (N=4 per group).

Figure 5: **Oxalate and oleic acid mediate IL-1α expression, release and surface expression on human monocytes**

A Western blot of human monocytes incubated with TNF-α (18 hours, 5 ng/mL), LPS (18 hours, 100 ng/mL), oxalate (4 hours, 100 µg/mL), oleic acid (OA, 4 hours, 100 µM) with or without LPS priming (18 hours, 100 ng/mL) to visualize pro-IL-1α and cleaved IL-1α in the cell lysate (representative of three independent experiments). **B** Release of IL-1α in the supernatant of monocytes stimulated as in **A** (N=3 per group). **** P<0.0001 for the comparison with untreated cells. **C** Expression of IL-1α on the surface of human monocytes stimulated as in **A** as determined by flow cytometry (representative of three independent experiments). **D** Release of IL-1α in the supernatant of monocytes stimulated as in **A** in the presence of the calcium chelators BAPTA-AM (10 µM), EGTA (2 mM) or the calpain inhibitors Z-Leu-Leu-CHO (1.2 µM), E-64-d (50 µg/mL, N=3 per group). *** P<0.001, **** P<0.0001 for the comparison to cells in the absence of the respective inhibitors.

Figure 6: **IL-1α on the surface of monocytes and IL-1R1 on the surface of endothelial cells mediate leukocyte-endothelial adhesion**

A Adhesion of DiI-labeled peripheral blood mononuclear cells (PBMCs) stimulated with either TNF-α (18 hours), LPS (18 hours), LPS+OA (18 hours for LPS priming, 4 hours), or LPS+Oxalate (18 hours for LPS priming, 4 hours) to human aortic endothelial cells (HAECs) as determined by fluorescence microscopy (N=3 per group) in the presence of an anti-IL-1α

blocking antibody (1 µg/mL) incubated with PBMCs or an anti-IL-1R1 blocking antibody incubated with HAECs (10 µg/mL) or an isotype control. **B** Vascular cell adhesion molecule-1 (VCAM-1) expression in HAECs stimulated with TNF-α (5 ng/mL) or increasing concentrations of IL-1α for 4 hours (N=3 per group) as determined by Western blot analyses. **C** VCAM-1 expression in HAECs stimulated with TNF-α, LPS, oxalate (Ox), LPS+Ox, oleic acid (OA), or LPS+OA for 4 hours (N=3 per group). **D** Adhesion of PBMCs from wildtype (WT) or *Il1a*$^{-/-}$ mice stimulated with LPS, LPS+OA, LPS+Ox to murine aortic endothelial cells (MAECs, N=3 per group). ** *P* <0.01, *** *P*<0.001, **** *P*<0.0001.

Figure 7: **IL-1α mediates inflammation after AMI**

A Outline of the left anterior descending (LAD) coronary artery ligation model in wildtype (WT) and *Il1a*$^{-/-}$ mice. **B** Expression of IL-1α in the myocardium of mice subjected to LAD ligation or sham operation three days after surgery (representative for four independent experiments). **C** HE staining of the heart three days after LAD ligation or sham surgery to visualize inflammatory cell infiltrates (representative for 5-7 independent experiments). **D-E** Myocardial accumulation of F4/80 macrophages and Ly6G neutrophils three days after LAD ligation or sham operation (representative for 5-7 independent experiments). Quantification is shown in **Supplemental Figure 2A-B**.

Figure 8: **IL-1α mediates kidney injury in an oxalate diet model**

A Outline of the mouse oxalate diet chronic kidney disease (CKD) model. **B-C** Serum creatinine and urea in wildtype and *Il1a*$^{-/-}$ mice subjected to oxalate diet (OX) or standard diet (SD) for two weeks (N=7-10 per group). **D** Quantification of kidney tissue fibrosis using Sirius Red staining in mice subjected to OX or SD for two weeks (N=7-10 per group). **E-F** Expression of F4/80 and Ly6G in kidneys of mice subjected to OX or SD for two weeks (N=7-10 per group).

Figure 1

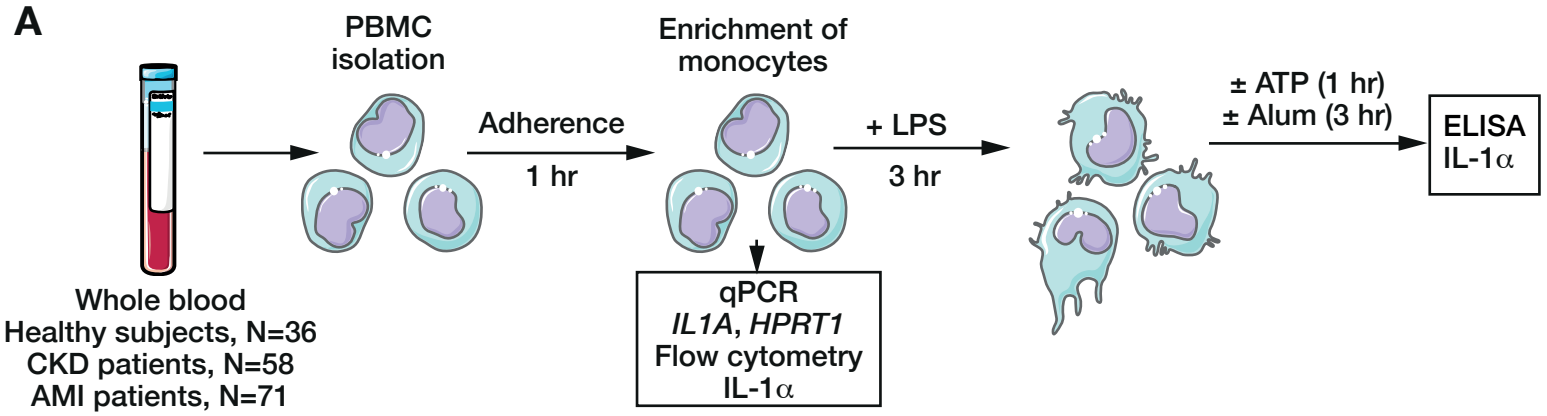
A
PBMC isolation
Enrichment of monocytes
Adherence
1 hr
+ LPS
3 hr
± ATP (1 hr)
± Alum (3 hr)
ELISA IL-1α
Whole blood
Healthy subjects, N=36
CKD patients, N=58
AMI patients, N=71
qPCR
IL1A, HPRT1
Flow cytometry
IL-1α

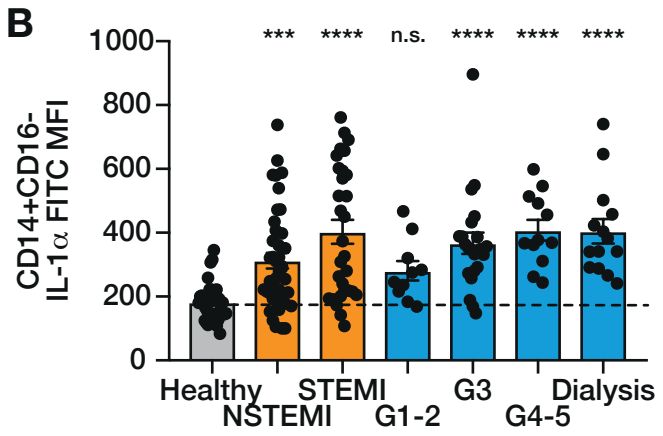
B
CD14+CD16- IL-1α FITC MFI
Healthy
STEMI
NSTEMI
G1-2
G3
G4-5
Dialysis

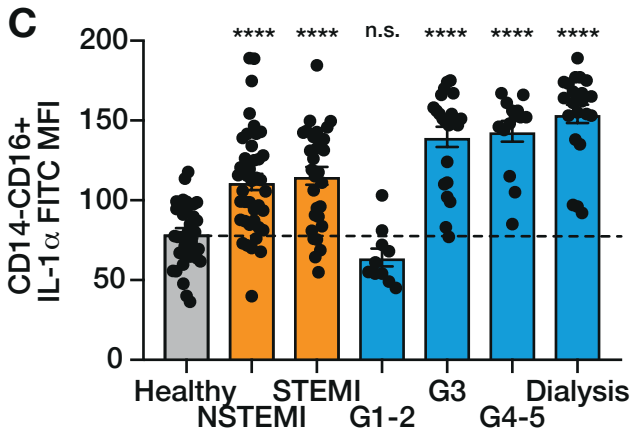
C
CD14-CD16+ IL-1α FITC MFI
Healthy
STEMI
NSTEMI
G1-2
G3
G4-5
Dialysis

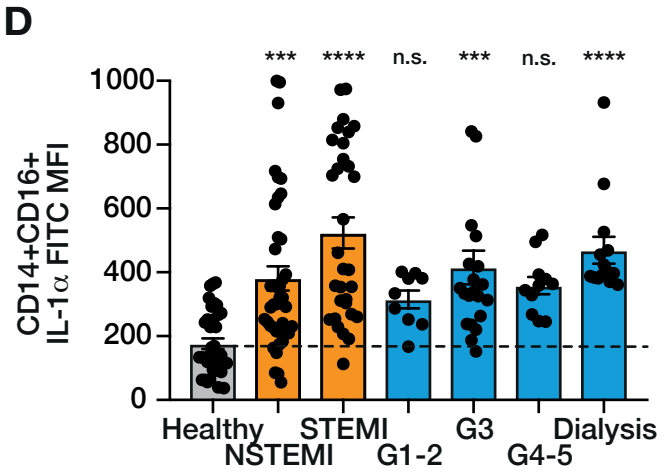
D
CD14+CD16+ IL-1α FITC MFI
Healthy
STEMI
NSTEMI
G1-2
G3
G4-5
Dialysis

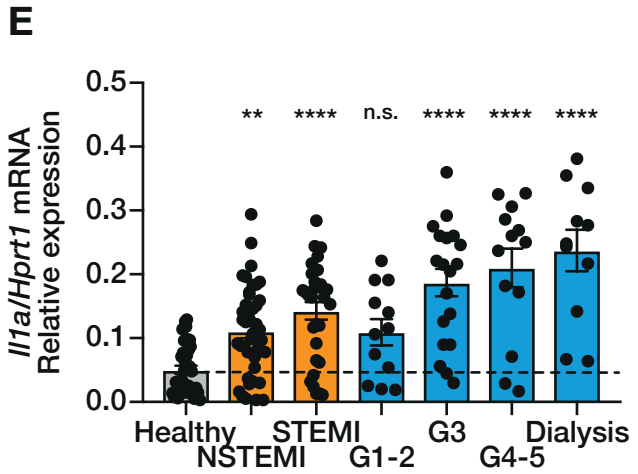
E
Il1a/Hprt1 mRNA Relative expression
Healthy
STEMI
NSTEMI
G1-2
G3
G4-5
Dialysis

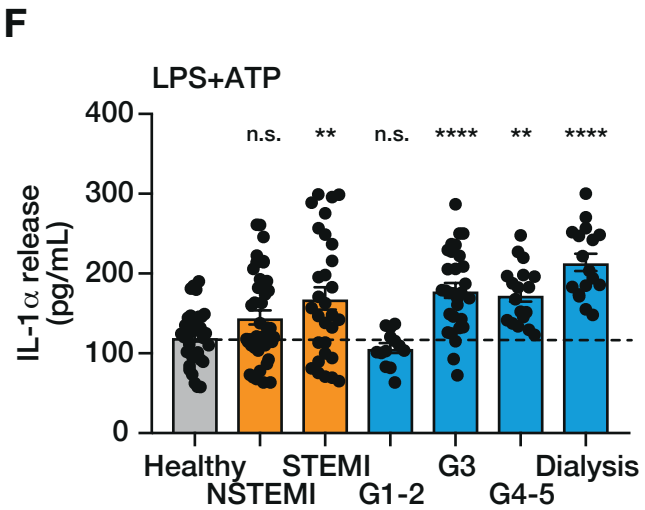
F
LPS+ATP
IL-1α release (pg/mL)
Healthy
STEMI
NSTEMI
G1-2
G3
G4-5
Dialysis

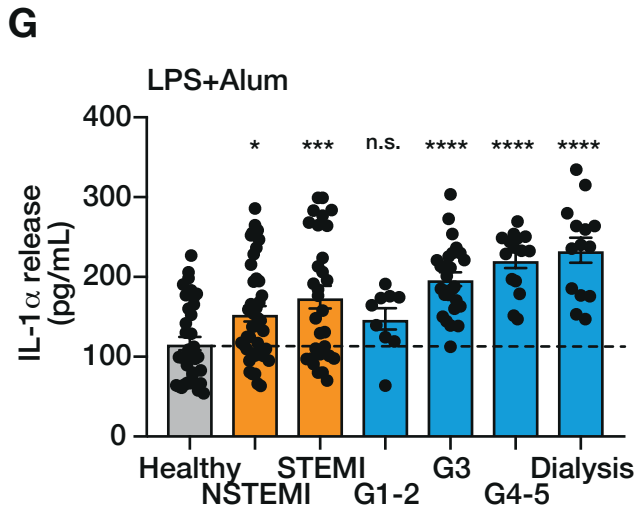
G
LPS+Alum
IL-1α release (pg/mL)
Healthy
STEMI
NSTEMI
G1-2
G3
G4-5
Dialysis

Figure 2

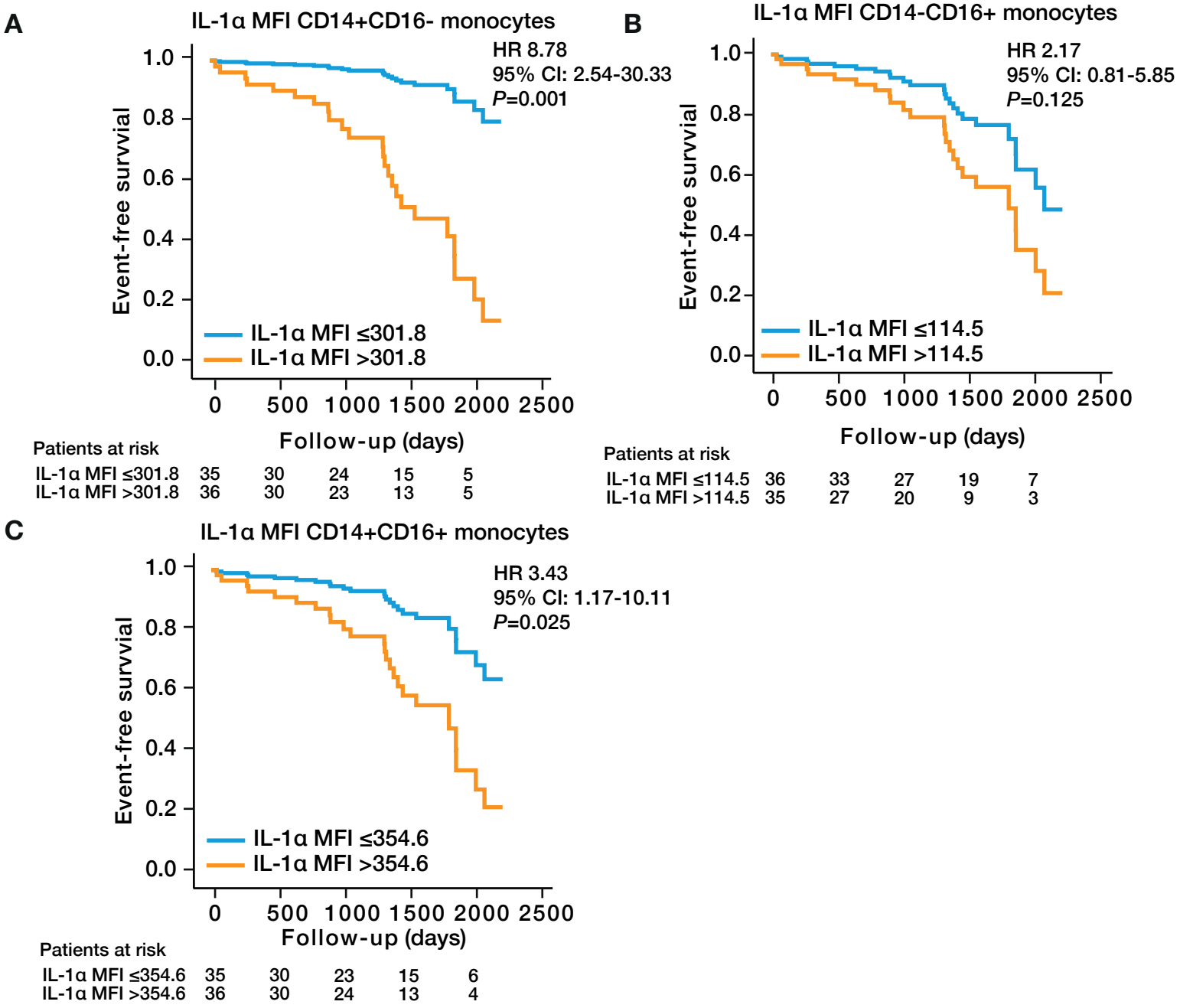
A
IL-1α MFI CD14+CD16- monocytes
HR 8.78
95% CI: 2.54-30.33
P=0.001
Event-free survvial
1.0
0.8
0.6
0.4
0.2
0.0
IL-1α MFI ≤301.8
IL-1α MFI >301.8
0
500
1000
1500
2000
2500
Follow-up (days)
Patients at risk
IL-1α MFI ≤301.8 35 30 24 15 5
IL-1α MFI >301.8 36 30 23 13 5
B
IL-1α MFI CD14-CD16+ monocytes
HR 2.17
95% CI: 0.81-5.85
P=0.125
Event-free survvial
IL-1α MFI ≤114.5
IL-1α MFI >114.5
Follow-up (days)
Patients at risk
IL-1α MFI ≤114.5 36 33 27 19 7
IL-1α MFI >114.5 35 27 20 9 3
C
IL-1α MFI CD14+CD16+ monocytes
HR 3.43
95% CI: 1.17-10.11
P=0.025
Event-free survvial
IL-1α MFI ≤354.6
IL-1α MFI >354.6
Follow-up (days)
Patients at risk
IL-1α MFI ≤354.6 35 30 23 15 6
IL-1α MFI >354.6 36 30 24 13 4

Figure 3

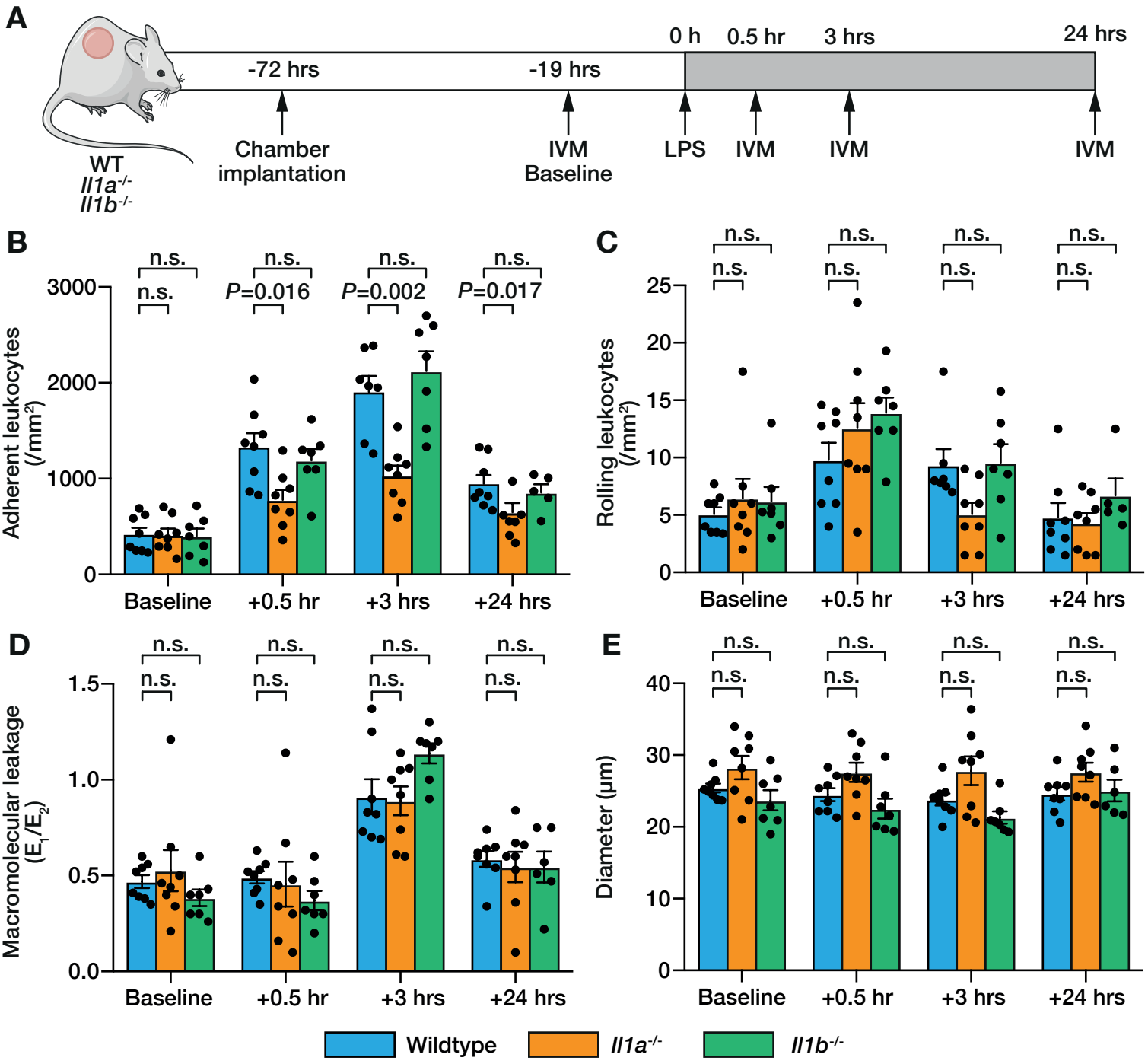
A
-72 hrs
-19 hrs
0 h
0.5 hr
3 hrs
24 hrs
Chamber implantation
IVM Baseline
LPS
IVM
IVM
IVM
WT
Il1a-/-
Il1b-/-
B
Adherent leukocytes (/mm2)
n.s.
P=0.016
P=0.002
P=0.017
Baseline
+0.5 hr
+3 hrs
+24 hrs
C
Rolling leukocytes (/mm2)
D
Macromolecular leakage (E1/E2)
E
Diameter (µm)
Wildtype
Il1a-/-
Il1b-/-

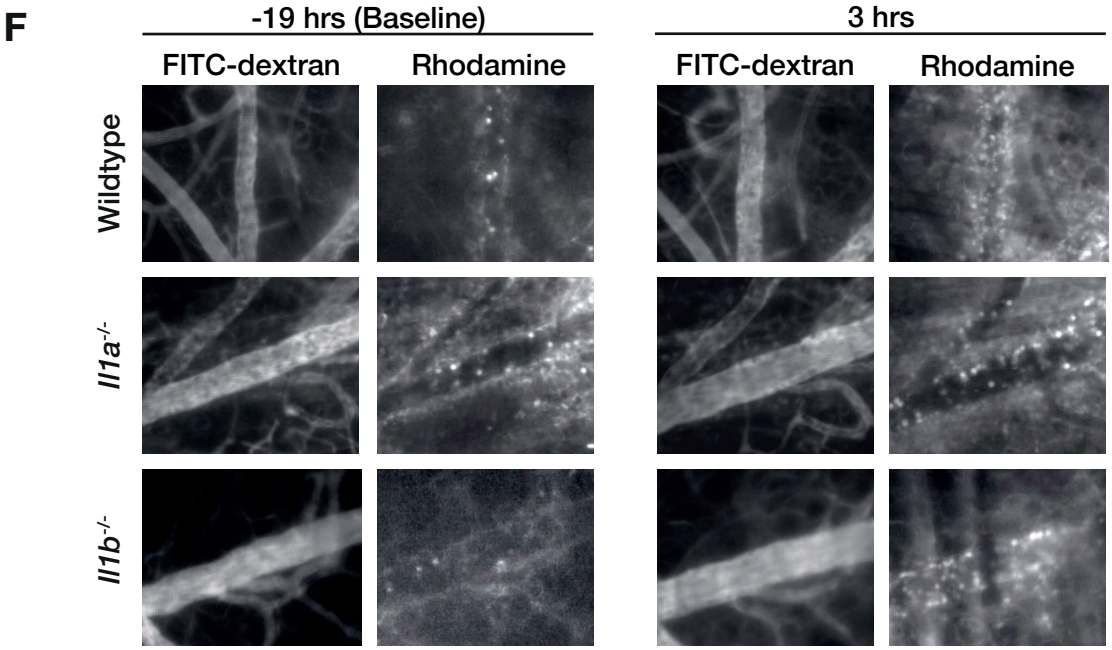
F
-19 hrs (Baseline)
3 hrs
FITC-dextran
Rhodamine
Wildtype
Il1a-/-
Il1b-/-

Figure 4

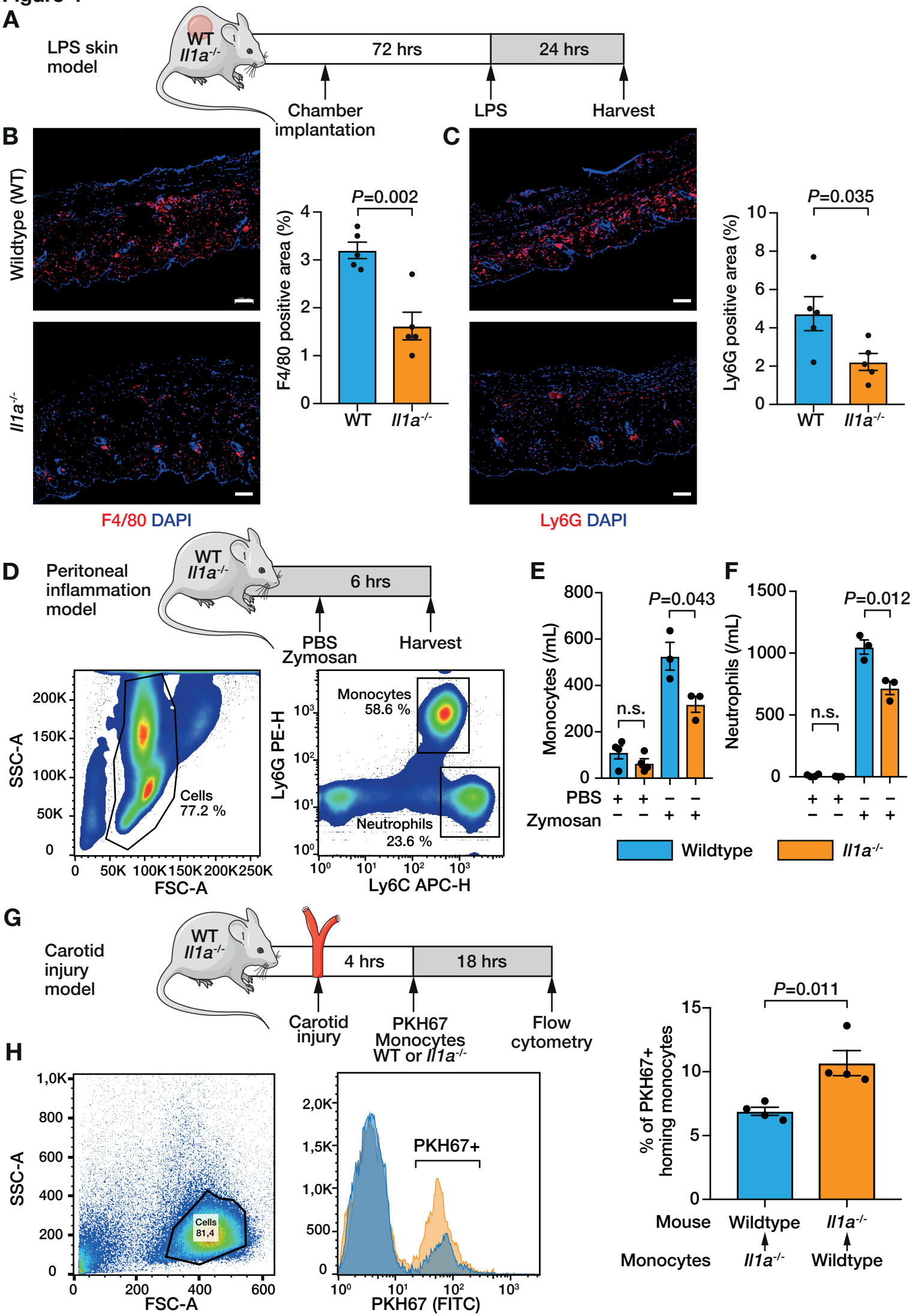
A
LPS skin model
WT
Il1a-/-
72 hrs
24 hrs
Chamber implantation
LPS
Harvest
B
Wildtype (WT)
Il1a-/-
F4/80 DAPI
P=0.002
F4/80 positive area (%)
WT
Il1a-/-
C
Ly6G DAPI
P=0.035
Ly6G positive area (%)
WT
Il1a-/-
D
Peritoneal inflammation model
WT
Il1a-/-
6 hrs
PBS
Zymosan
Harvest
SSC-A
FSC-A
Cells
77.2 %
Ly6G PE-H
Ly6C APC-H
Monocytes
58.6 %
Neutrophils
23.6 %
E
P=0.043
Monocytes (/mL)
n.s.
PBS
Zymosan
F
P=0.012
Neutrophils (/mL)
n.s.
Wildtype
Il1a-/-
G
Carotid injury model
WT
Il1a-/-
4 hrs
18 hrs
Carotid injury
PKH67 Monocytes WT or Il1a-/-
Flow cytometry
H
SSC-A
FSC-A
Cells
81,4
PKH67+
PKH67 (FITC)
P=0.011
% of PKH67+ homing monocytes
Mouse
Wildtype
Il1a-/-
Monocytes
Il1a-/-
Wildtype

Figure 5

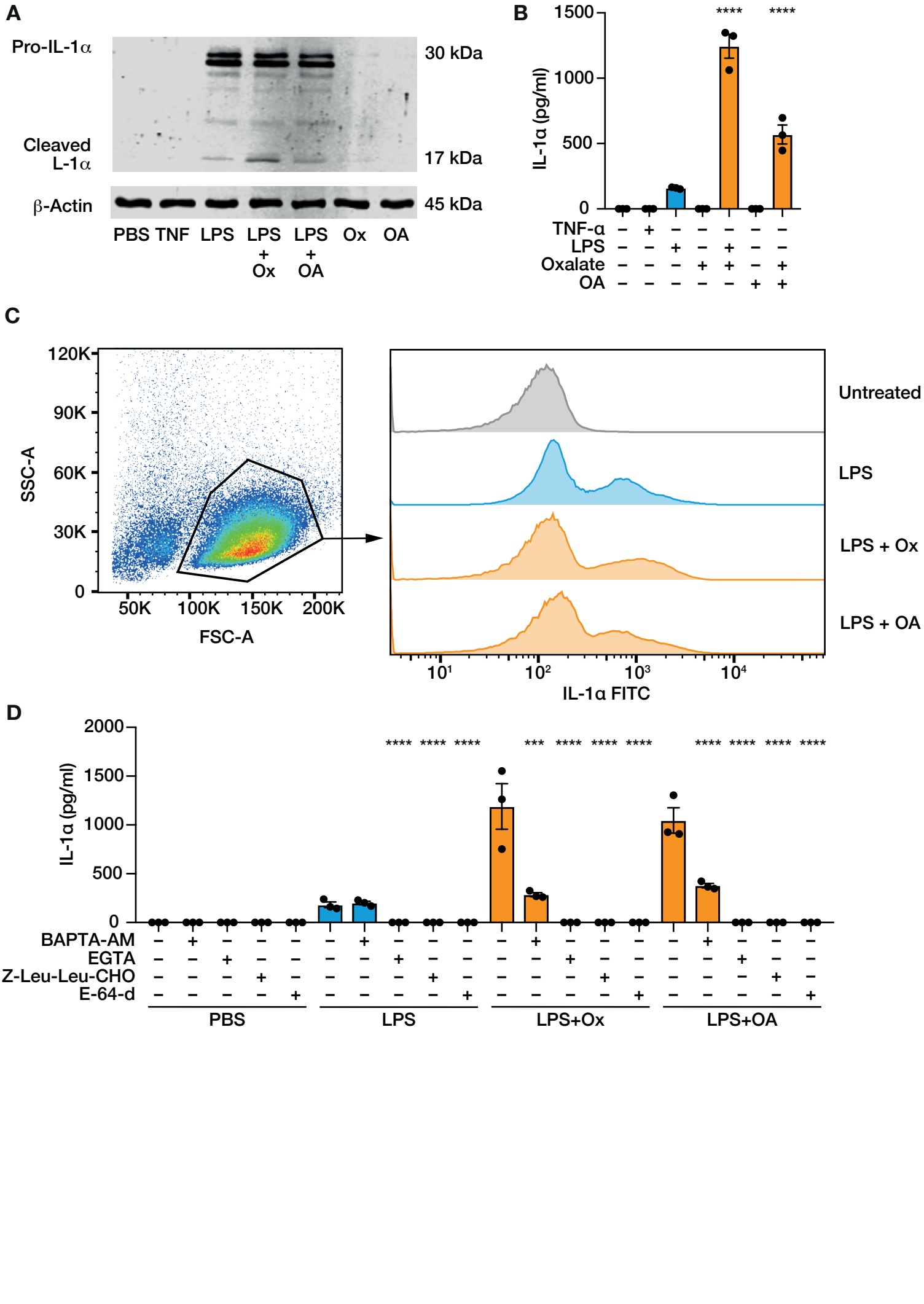
A
Pro-IL-1α
Cleaved L-1α
β-Actin
30 kDa
17 kDa
45 kDa
PBS TNF LPS LPS + Ox LPS + OA Ox OA
B
IL-1α (pg/ml)
1500
1000
500
0
****
****
TNF-α
LPS
Oxalate
OA
C
120K
90K
60K
30K
0
SSC-A
50K
100K
150K
200K
FSC-A
Untreated
LPS
LPS + Ox
LPS + OA
10¹
10²
10³
10⁴
IL-1α FITC
D
IL-1α (pg/ml)
2000
1500
1000
500
0
BAPTA-AM
EGTA
Z-Leu-Leu-CHO
E-64-d
PBS
LPS
LPS+Ox
LPS+OA

Figure 6

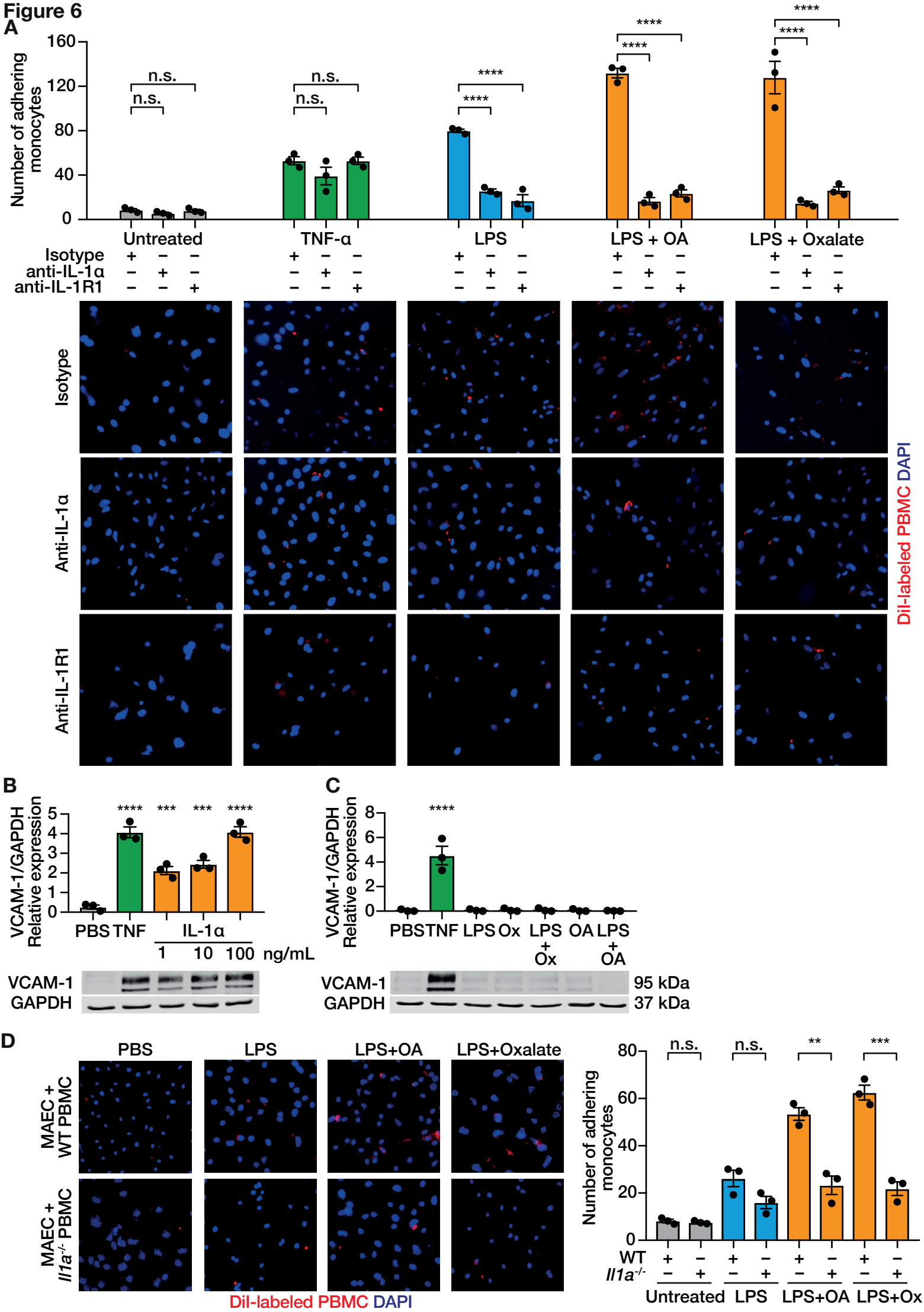
A
Number of adhering monocytes
160
120
80
40
0
n.s.
n.s.
n.s.
n.s.
****
****
****
****
****
****
Untreated
TNF-α
LPS
LPS + OA
LPS + Oxalate
Isotype + − − + − − + − − + − − + − −
anti-IL-1α − + − − + − − + − − + − − + −
anti-IL-1R1 − − + − − + − − + − − + − − +
Isotype
Anti-IL-1α
Anti-IL-1R1
DiI-labeled PBMC DAPI
B
VCAM-1/GAPDH Relative expression
5
4
3
2
1
0
****
***
***
****
PBS TNF IL-1α
1 10 100 ng/mL
VCAM-1
GAPDH
C
VCAM-1/GAPDH Relative expression
8
6
4
2
0
****
PBS TNF LPS Ox LPS + Ox OA LPS + OA
VCAM-1
GAPDH
95 kDa
37 kDa
D
PBS
LPS
LPS+OA
LPS+Oxalate
MAEC + WT PBMC
MAEC + Il1a-/- PBMC
DiI-labeled PBMC DAPI
Number of adhering monocytes
80
60
40
20
0
n.s.
n.s.
**
***
WT + − + − + − + −
Il1a-/- − + − + − + − +
Untreated LPS LPS+OA LPS+Ox

Figure 7

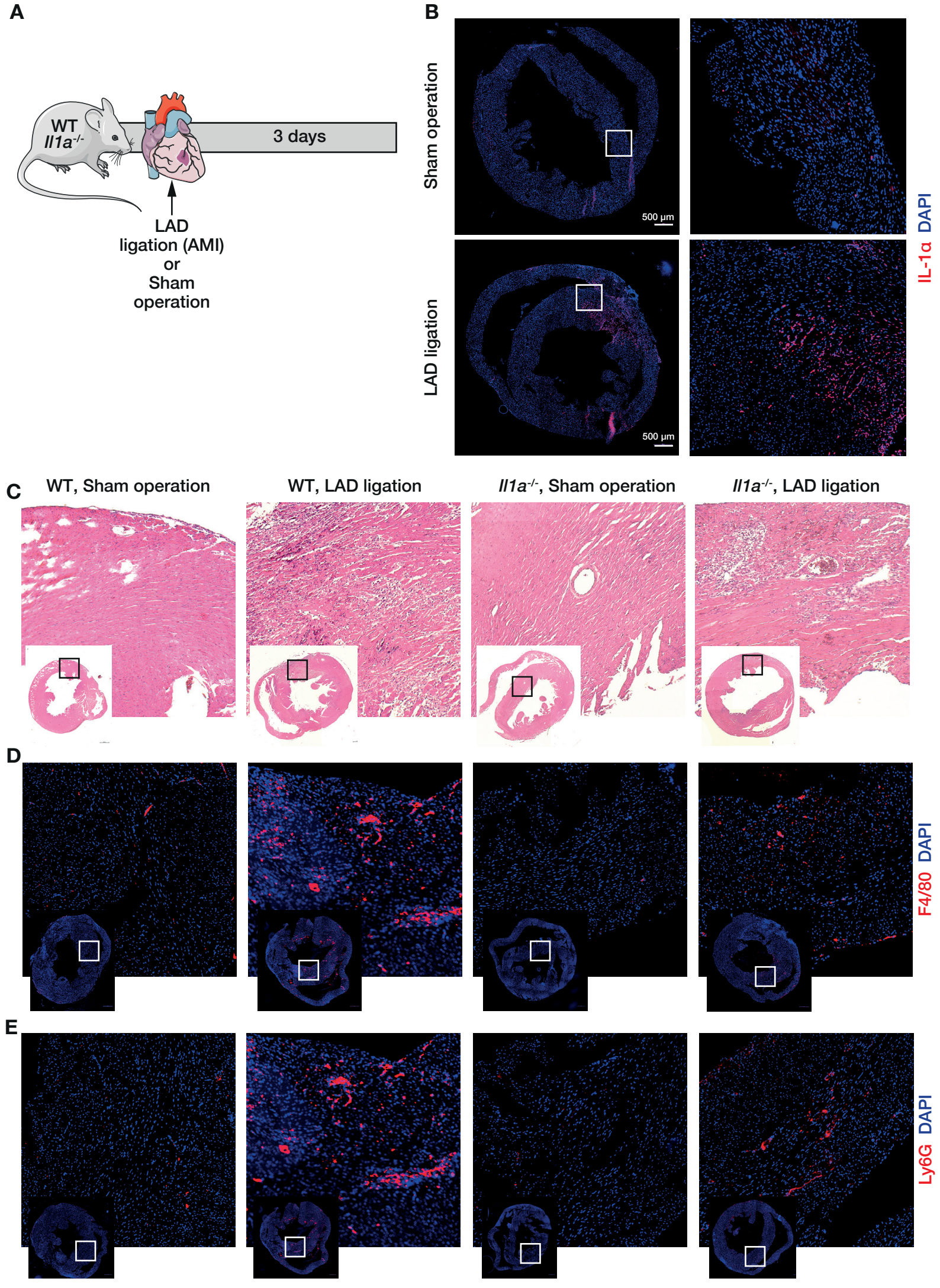
A
WT
Il1a-/-
3 days
LAD
ligation (AMI)
or
Sham
operation
B
Sham operation
LAD ligation
500 μm
500 μm
IL-1α DAPI
C
WT, Sham operation
WT, LAD ligation
Il1a-/-, Sham operation
Il1a-/-, LAD ligation
D
F4/80 DAPI
E
Ly6G DAPI

Figure 8

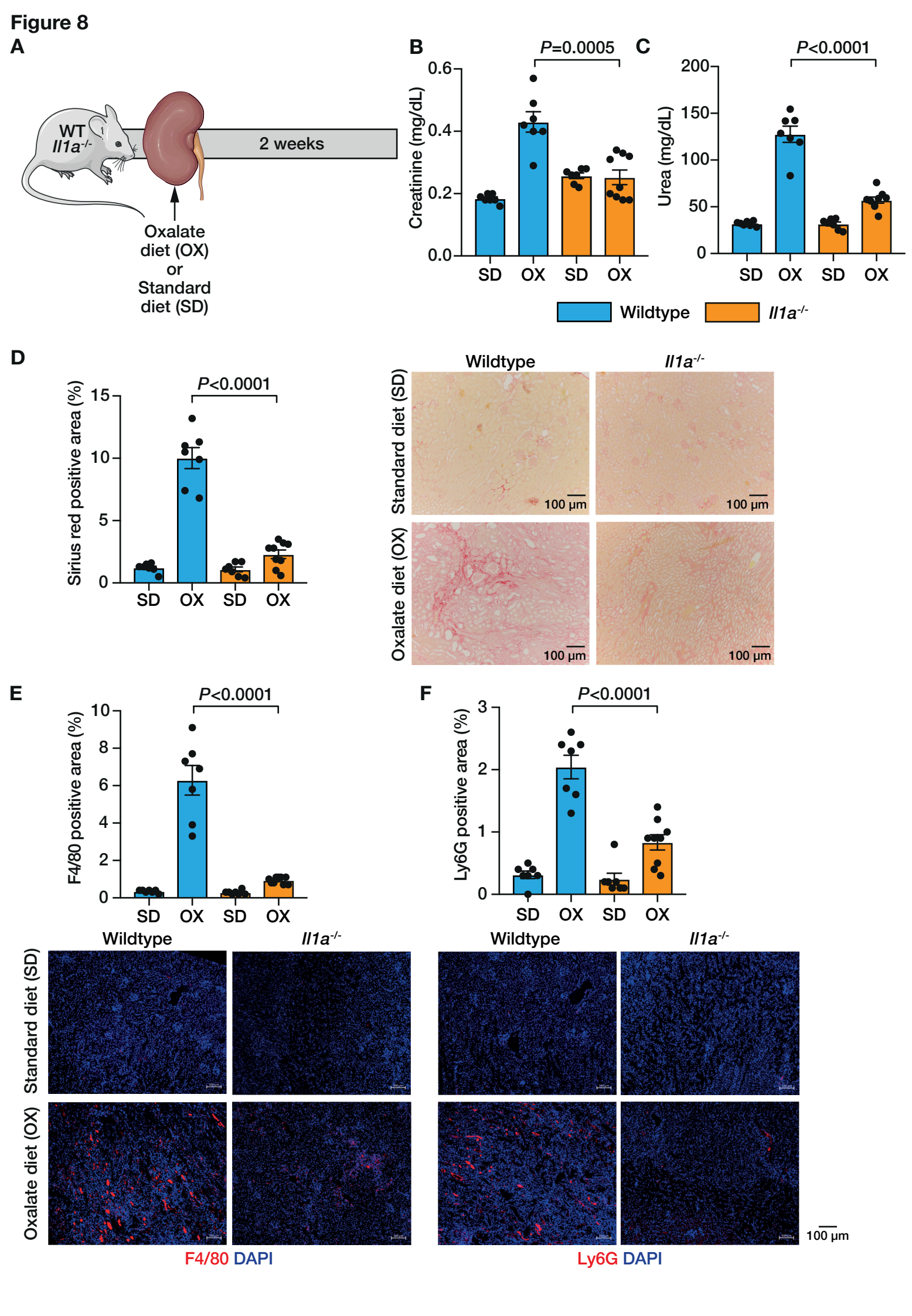
A
WT
Il1a-/-
2 weeks
Oxalate diet (OX) or Standard diet (SD)
B
P=0.0005
Creatinine (mg/dL)
0.6
0.4
0.2
0.0
SD
OX
SD
OX
C
P<0.0001
Urea (mg/dL)
200
150
100
50
0
SD
OX
SD
OX
Wildtype
Il1a-/-
D
P<0.0001
Sirius red positive area (%)
15
10
5
0
SD
OX
SD
OX
Wildtype
Il1a-/-
Standard diet (SD)
Oxalate diet (OX)
100 µm
E
P<0.0001
F4/80 positive area (%)
10
8
6
4
2
0
SD
OX
SD
OX
F
P<0.0001
Ly6G positive area (%)
3
2
1
0
SD
OX
SD
OX
Wildtype
Il1a-/-
Standard diet (SD)
Oxalate diet (OX)
100 µm
F4/80 DAPI
Ly6G DAPI

Supplementary figure 1

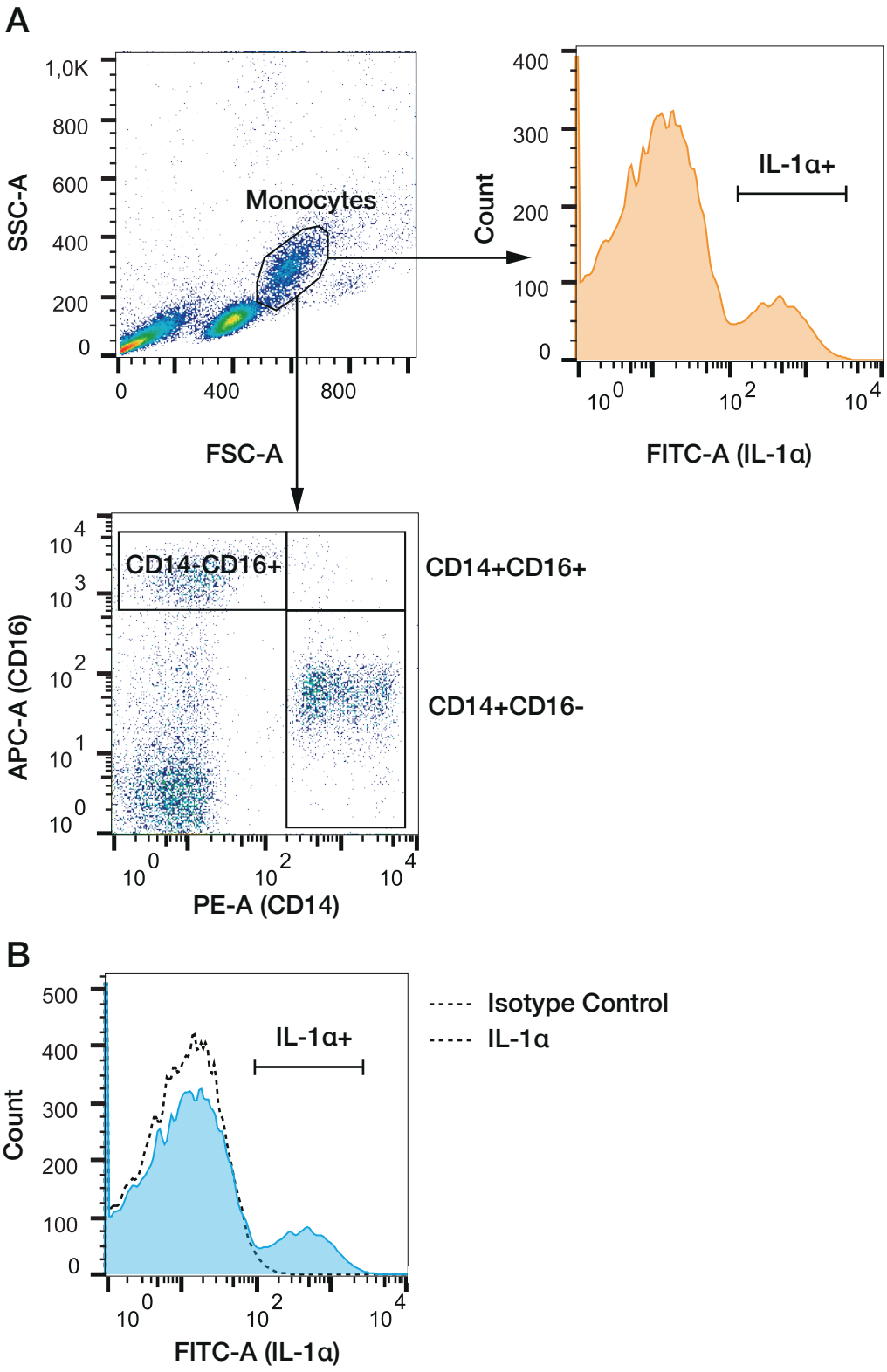

Supplementary figure 2

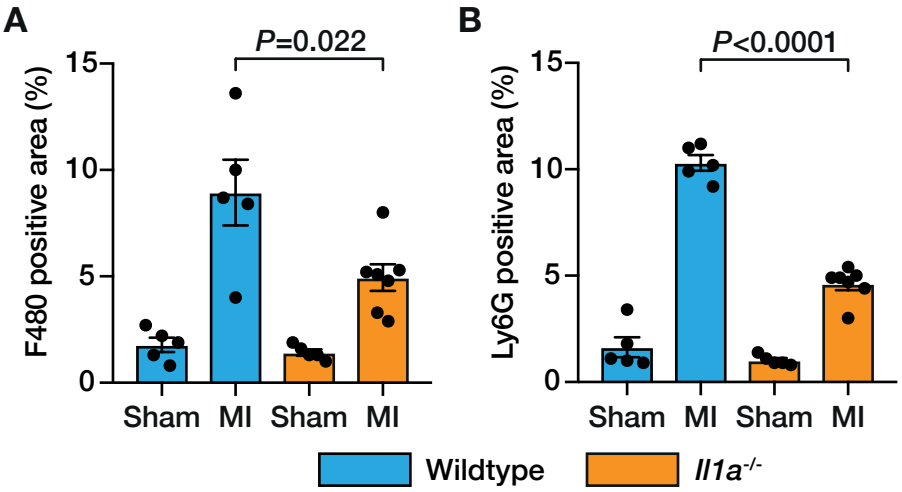

Supplementary figure 3

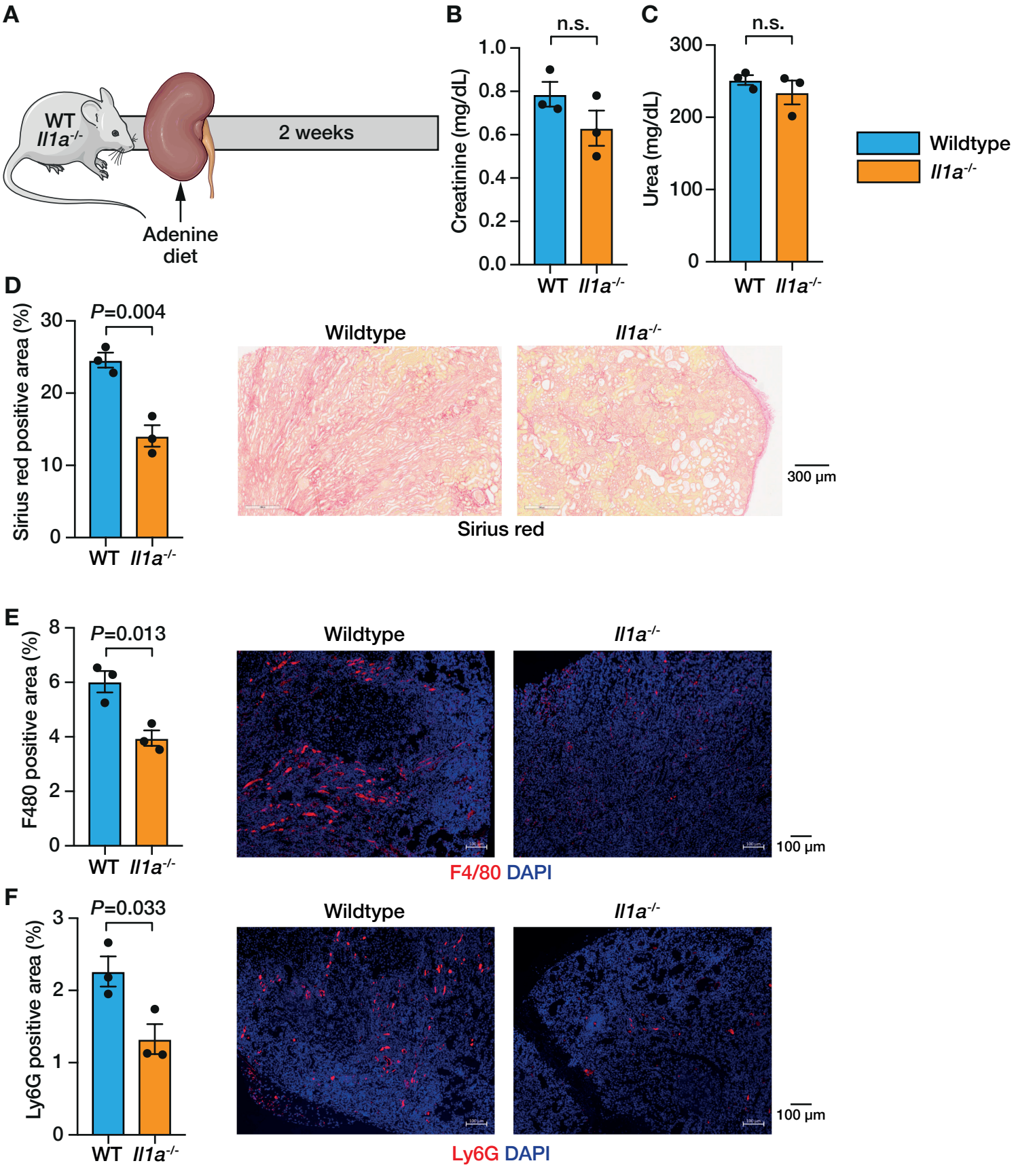

Supplementary figure 4

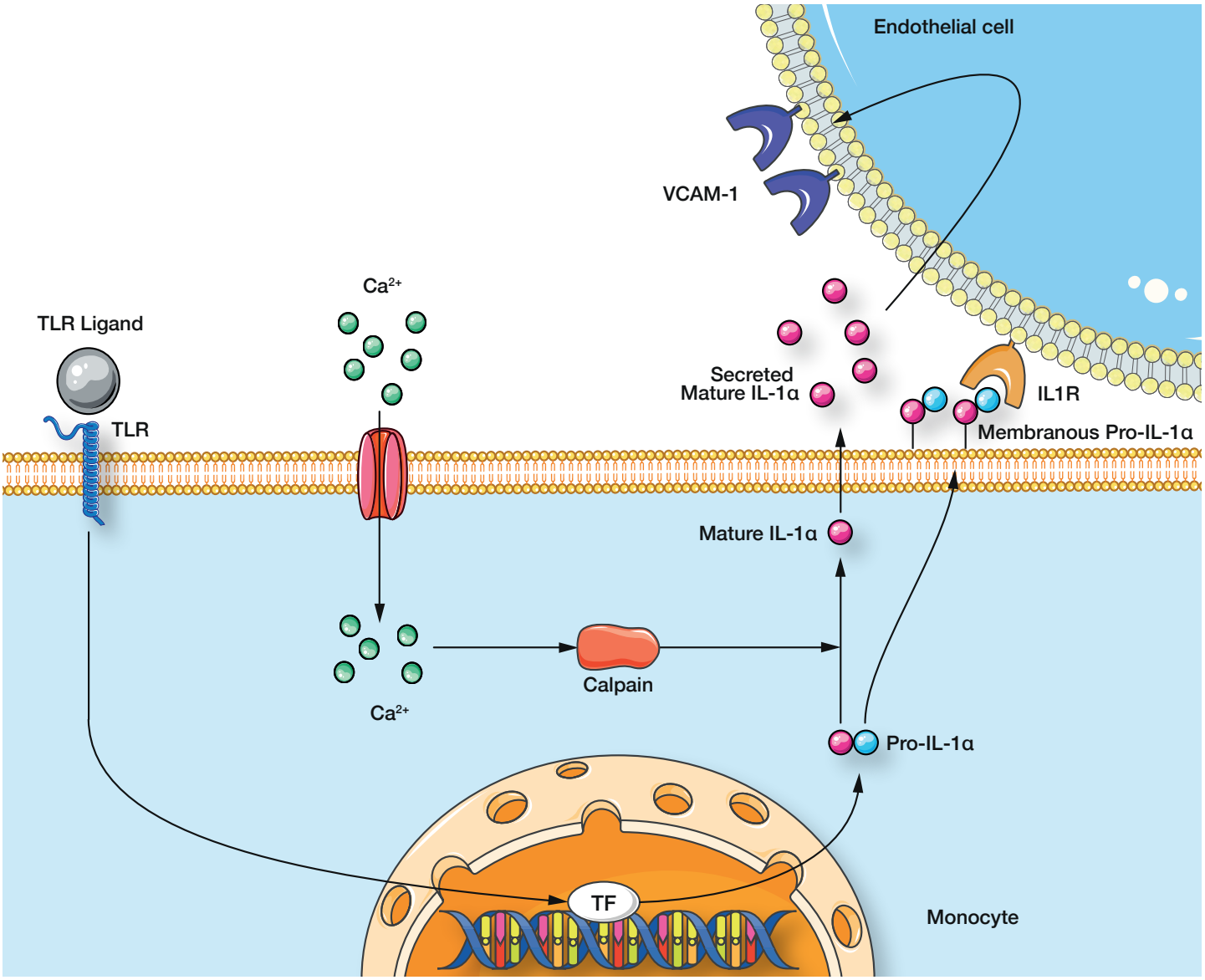

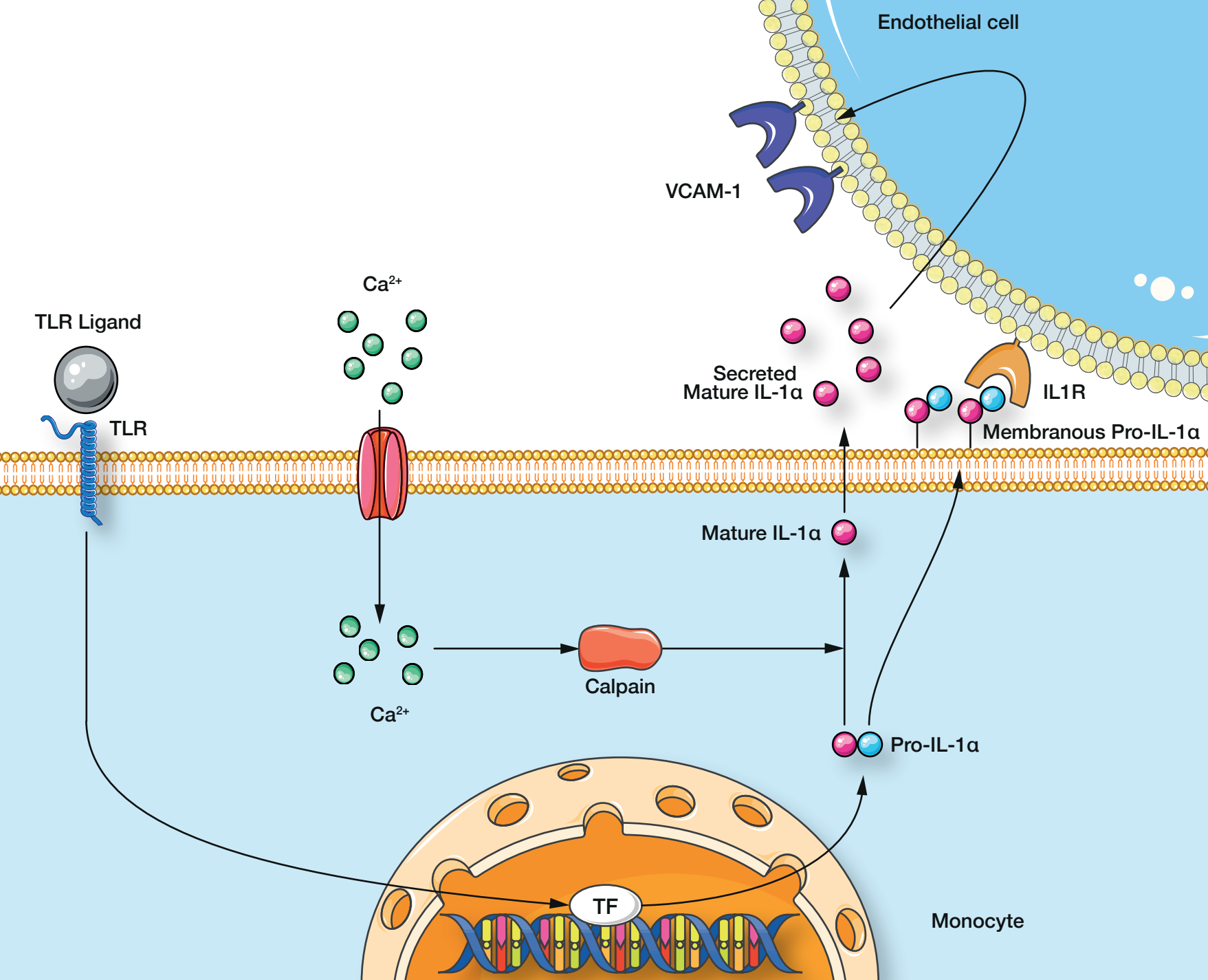
Endothelial cell
VCAM-1
Ca2+
TLR Ligand
TLR
Secreted
Mature IL-1α
IL1R
Membranous Pro-IL-1α
Mature IL-1α
Calpain
Ca2+
Pro-IL-1α
TF
Monocyte